

# Asymmetric Penalties Underlie Proper Loss Functions in Probabilistic Forecasting

Erez Buchweitz

João Vitor Romano

Ryan J. Tibshirani

## Abstract

Accurately forecasting the probability distribution of phenomena of interest is a classic and ever more widespread goal in statistics and decision theory. In comparison to point forecasts, probabilistic forecasts aim to provide a more complete and informative characterization of the target variable. This endeavor is only fruitful, however, if a forecast is “close” to the distribution it attempts to predict. The role of a loss function—also known as a scoring rule—is to make this precise by providing a quantitative measure of proximity between a forecast distribution and target random variable. Numerous loss functions have been proposed in the literature, with a strong focus on proper losses, that is, losses whose expectations are minimized when the forecast distribution is the same as the target. In this paper, we show that a broad class of proper loss functions penalize *asymmetrically*, in the sense that underestimating a given parameter of the target distribution can incur larger loss than overestimating it, or vice versa. Our theory covers many popular losses, such as the logarithmic, continuous ranked probability, quadratic, and spherical losses, as well as the energy and threshold-weighted generalizations of continuous ranked probability loss. To complement our theory, we present experiments with real epidemiological, meteorological, and retail forecast data sets. Further, as an implication of the loss asymmetries revealed by our work, we show that hedging is possible under a setting of distribution shift.

## 1 Introduction

In probabilistic forecasting, the goal is to predict the distribution of a target variable, rather than a particular parameter of that distribution, such as its mean or a single quantile, which is termed point forecasting. The pursuit of probabilistic forecasts has been promoted based on philosophical grounds, as an adequate form of expressing the inherent uncertainty in predicting the target variable (Dawid, 1984; Gneiting and Raftery, 2007). From a practical viewpoint, a probabilistic forecast provides more detailed information on the possible realizations of the target, which is generally considered useful for decision making (Jordan et al., 2011; Jolliffe and Stephenson, 2012; Cramer et al., 2022b). Accordingly, in various scientific disciplines, probabilistic forecasts are widespread and growing in use (Gneiting and Katzfuss, 2014), with some examples being the prediction of floods (Pappenberger et al., 2011), earthquakes (Schorlemmer et al., 2018), epidemics (Cramer et al., 2022b), energy usage (Hong et al., 2016), population growth (Raftery and Ševčíková, 2023), and inflation (Galbraith and van Norden, 2012).

Loss functions measure the discrepancy between a prediction and an observed target. In probabilistic forecasting, each prediction is an entire probability distribution, whereas the target is a random variable. Hence, a loss function assigns a numeric value to the discrepancy between a real value (in case the target variable is real) and a probability distribution from which it has purportedly originated. The study of loss functions—commonly called scoring rules in probabilistic forecasting—originated in weather forecasting (Brier, 1950; Winkler and Murphy, 1968; Matheson and Winkler, 1976), intertwined with the development of subjective probability (Good, 1952; de Finetti, 1975; Savage, 1971), and has largely revolved around propriety. A loss function is deemed proper if the least loss, in expectation over all possible realizations of the target, is incurred when the forecast equals the distribution of the target (Gneiting and Raftery, 2007).

It is commonly held that proper losses encourage “honest forecasting” (Gneiting and Raftery, 2007; Parry et al., 2012); formally, this is guaranteed only in the special (rare) case that the forecaster knows *with certainty* what the distribution of the target is, as then they can do no better than to forecast it. In any case, this forms the basis of the wide appeal and subsequently the wide prevalence of proper losses, in both theory and practice.

A practitioner looking to fit or evaluate probabilistic forecasts must choose which loss function to optimize. For instance, it is common to fit a forecasting model by minimizing the average loss over a training set (Rasp and Lerch, 2018), or to

choose from among a collection of forecasts by minimizing the average loss on a test set (Cramer et al., 2022b). Dawid (2007) lays out a method for constructing proper losses in which propriety is tied to Bayes (optimal) actions in a given decision-making task. However, it remains that practitioners largely prefer to choose one out of a plethora of losses that have been proposed in the literature for general purpose, or a combination thereof (as exhibited in the domain-focused references on forecasting given previously). In the absence of a definitive theory as to which loss is preferable in a given situation, some authors have recommended choosing one whose well-known properties appear to be aligned with the use case (Winkler et al., 1996; Gneiting and Raftery, 2007). The study of the properties of each particular loss function has therefore become a major theme in probabilistic forecasting, and we contribute to this literature by characterizing *asymmetries*: which forecasting errors are awarded lesser or greater loss, by particular loss functions.

By definition, any proper loss function will favor the true distribution of the target by awarding it the minimal loss, on average over all possible realizations of the target. But in practice, forecasts are rarely equal to the true distribution of the target due to model misspecification, distribution shift and for other reasons. Which forecast will then be awarded the least expected loss depends on how a particular loss function penalizes different kinds of errors. Figure 1 displays the expected loss when the forecast and target distribution are both normal, for two of the most commonly used loss functions in practice. Given a choice between two forecasts where the forecast variance is either double or half the target variance, *logarithmic loss* will favor doubling the variance, choosing a flat, less informative forecast, while *continuous ranked probability (CRP) loss* will favor halving the variance, providing for a sharp overconfident forecast. (In both cases the mean is correctly specified. For definitions of those and other loss functions, see Section 2.)

The same findings can be recreated on real data from the Covid-19 Forecast Hub (Cramer et al., 2022a), as shown in Figure 2. (For details on the experimental setup, see Section 4.) We highlight another effect appearing in the left-most plot in Figure 2: given a choice between two forecasts, either shifted upward by one unit, or shifted downward by the same amount, logarithmic loss will favor the downshifted forecast. We attribute this asymmetry effect particularly to right-skewed forecasts, which Covid-19 mortality distributions typically are. Finally, notice in Figure 2 that the target mean and variance do not minimize logarithmic loss. This is because the forecast location-scale family is misspecified, meaning that it does not equal the target location-scale family. A setting of misspecification in which minimizers of loss deviate from the target is studied analytically in Section 5, and further research is warranted.

The effects described above may lead, among other things, to:

1. Chosen forecasts having a systematic tendency to be overly flat, sharp, or shifted, depending on the loss function used to choose them;
2. Forecasters being incentivized to report overly flat, sharp, or shifted forecasts, again depending on the loss used to evaluate them.

The first consequence above is demonstrated in Figures 3 and 4, which depict results on real data from the Covid-19 Forecast Hub and the M5 Uncertainty Competition (Makridakis et al., 2022), respectively. In both cases, forecasters with high standardized variance (meaning that they produced relatively flat forecasts) were generally ranked at least as high under logarithmic loss (meaning that they received relatively low loss) as under CRP loss. Conversely, CRP loss generally ranked forecasters with low standardized variance at least as high as logarithmic loss did. Practitioners ought to be aware of the asymmetries described in this paper pertaining to these and other commonly used loss functions. The choice of loss function can affect the ranking of forecasts in predictable ways. The second of the consequences above, detailing incentives imposed upon the forecasters by different loss functions, is discussed in Section 5.

## 1.1 Summary of main results

We now summarize the main results of this paper, on asymmetries inherent to logarithmic, CRP, quadratic, spherical, energy, and Dawid–Sebastiani (DS) losses (Section 2 gives their definitions). We denote by  $\ell(F, G)$  the expected loss when  $F$  is the forecast and  $G$  is the target distribution. Our first main result (Section 3.1), pertains to scale families.

**Theorem 1** (Scale family). *Let  $\{G_\sigma : \sigma > 0\}$  be a scale family. Fix  $G = G_1$  and  $\sigma > 1$ . The following holds.*

- For CRP and energy losses,  $\ell(G_\sigma, G) > \ell(G_{1/\sigma}, G)$ .
- For quadratic and DS losses,  $\ell(G_\sigma, G) < \ell(G_{1/\sigma}, G)$ .
- For spherical loss,  $\ell(G_\sigma, G) = \ell(G_{1/\sigma}, G)$ .

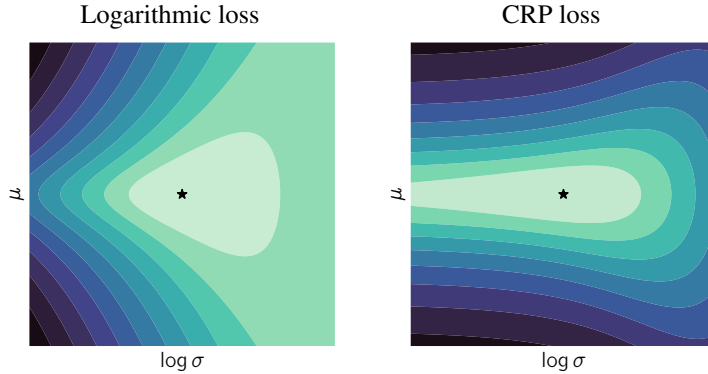


Figure 1: Expected logarithmic and CRP losses for a fixed standard normal target and normal forecasts with varying location  $\mu$  and scale  $\sigma$ . A lighter color represents a lower loss, with minimum achieved at the star, where the forecast distribution is also a standard normal. When the location is correctly specified, logarithmic loss penalizes underestimating the scale more than overestimating it, whereas the opposite is true for CRP. When the scale is correctly specified, both losses penalize symmetrically on the location.

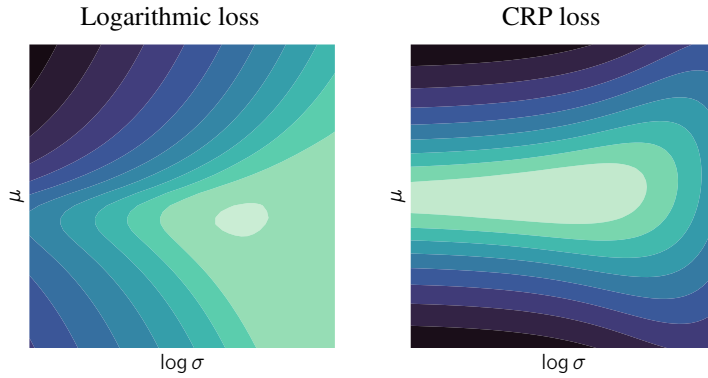


Figure 2: Average logarithmic and CRP losses over targets and forecasts from the Covid-19 Forecast Hub (for details see Section 4). The qualitative assessment for CRP loss is exactly the same as in the normal case; for logarithmic loss there is an additional location asymmetry that is due to the forecasts being right-skewed.

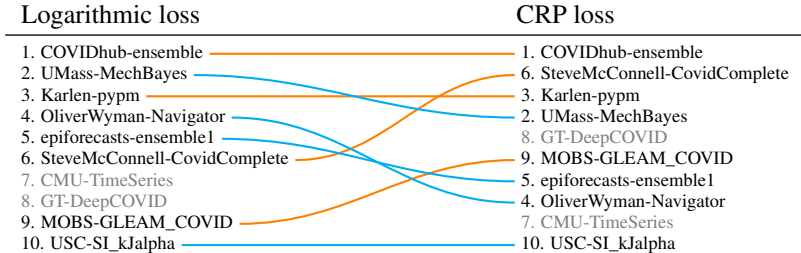


Figure 3: Ranking of top forecasters in the Covid-19 Forecast Hub via logarithmic and CRP losses. Each line connects the same forecaster over the two ranked lists, and orange (cyan) lines identify the forecasters with lowest (highest) standardized variance.

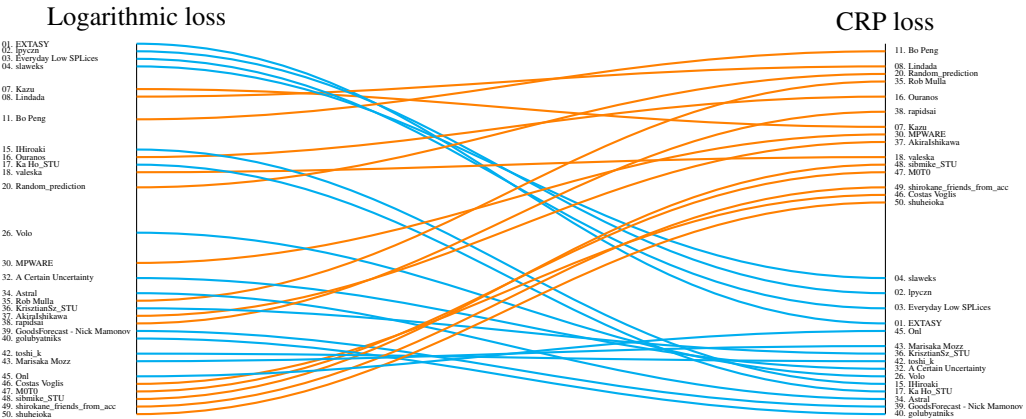


Figure 4: Ranking of top forecasters in the M5 Uncertainty Competition via logarithmic and CRP losses. Lines again connect the same forecasters over the ranked lists, and orange (cyan) lines identify the forecasters with lowest (highest) standardized variance.

Supposing the target variable  $Y$  follows a distribution  $G$ , we define  $G_\sigma$  as the distribution of  $\sigma Y$ . For CRP and energy losses, the expected loss is larger when forecasting  $G_\sigma$  versus  $G_{1/\sigma}$  for any value of  $\sigma > 1$ . Recalling  $G = G_1$ , these loss functions thus favor underestimating the scale parameter compared to overestimating it by the same amount, on a logarithmic scale. In other words, facing a choice between a flat, less informative forecast  $G_\sigma$  and a sharp overconfident forecast  $G_{1/\sigma}$ , CRP and energy losses will always favor the latter, regardless of the particular scale family. Conversely, quadratic and DS losses will always favor the former: the flat, less informative forecast in a scale family. Spherical loss will favor neither, however this should not be taken at face value, as will become clearer later. For threshold-weighted CRP loss, the asymmetry depends on the weight function (see Section 6.3). We find Theorem 1 in agreement with the empirical findings in Figure 1. Importantly, Figure 2 presents empirical evidence that a similar phenomenon can occur when the forecast and target distribution are not of the same family.

Logarithmic loss is notably absent from Theorem 1. For this loss, the direction of asymmetry may differ between scale families. Our second main result (Section 3.3) characterizes the asymmetry inherent to logarithmic loss, with respect to exponential families.

**Theorem 2** (Exponential family). *Let  $\{G_\theta : \theta > 0\}$  be a minimal exponential family. Fix  $G = G_1$ ,  $\theta > 1$ , and denote by  $\ell$  the logarithmic loss. The following holds.*

- *If the family is a normal, exponential, Laplace, Weibull, or (generalized) gamma scale family, or a log-normal log-scale family, then  $\ell(G_\theta, G) < \ell(G_{1/\theta}, G)$ .*
- *If the family is an inverse gamma scale family, then  $\ell(G_\theta, G) > \ell(G_{1/\theta}, G)$ .*
- *If the family is a (generalized) gamma, Pareto, inverse Gaussian, or beta shape family, or a Poisson rate family, then  $\ell(G_\theta, G) > \ell(G_{1/\theta}, G)$ .*

In most (but not all) of the examples of scale families that we were able to find, logarithmic loss favors overestimating the scale rather than underestimating it by the same amount, on a logarithmic scale as before. This is in agreement with Figure 1 (which examines the normal case) and 2 (the misspecified case where  $F, G$  are not of the same family). The converse is true for exponential families with so-called shape parameters, typically right-skewed, in which logarithmic loss favors underestimating the shape. We believe the empirical results pertaining to asymmetry in right-skewed location families, which are favored underestimated in Figure 2, may be understood in this light.

We complement the above results on scale and exponential families with a result on location families.

**Theorem 3** (Location family). *Let  $\{G_\mu : \mu \in \mathbb{R}\}$  be a location family. Fix  $G = G_0$ . The following holds.*

- *For CRP, quadratic, spherical, energy, and DS losses,  $\ell(G_\mu, G) = \ell(G_{-\mu}, G)$ .*
- *For logarithmic loss,  $\ell(G_\mu, G) = \ell(G_{-\mu}, G)$ , provided  $G$  is symmetric.*

Supposing the target variable  $Y$  follows a distribution  $G$ , we define  $G_\mu$  as the distribution of  $Y + \mu$ . CRP, quadratic, spherical, energy, and DS losses do not favor underestimating nor overestimating the location, in any location family. Logarithmic loss behaves the same way, provided  $G$  is symmetric. For threshold-weighted CRP loss, the asymmetry depends on the weight function (see Section 6.3). These results are in line with Figure 1, and Figure 2 again provides empirical evidence that the same can be true when the forecast and target distribution are not of the same family (recall, the asymmetry for logarithmic loss with respect to location can be interpreted via Theorem 2).

The results in Theorems 1–3 still hold when we replace each  $\ell(F, G)$  by the divergence  $d(F, G) = \ell(F, G) - \ell(G, G)$ . Common proper losses induce well-known divergences, such as the Kullback–Leibler divergence (which is induced by logarithmic loss), Cramér distance (CRP loss), energy distance (energy loss),  $L^2$  distance between densities (quadratic loss), and so on. These divergences are widely-used in probability, statistics, and many application areas. Therefore, a characterization of asymmetries, as we give in this paper, may be of interest outside of probabilistic forecasting.

## 1.2 Structure of this paper

The rest of this paper is structured as follows. In Section 2, we formally introduce the setting of probabilistic forecasting and the loss functions that are discussed in this paper. In Section 3, we derive our main theoretical results regarding asymmetric penalties. In Section 4, we present empirical analyses of three real data sets, as well as synthetic data. In

Section 5, we leverage our results to shed light on hedging proper loss functions under distribution shift. In Section 6, we conclude with a discussion of our findings, some assorted additional results, and ideas for future work.

### 1.3 Related literature

References to the broader literature on proper losses will be given in the next section, and here we restrict our attention to literature more narrowly adjacent to the focus of our paper. We are of course not the first to consider the operating characteristics of proper losses, and how this might influence the choice of which loss to use. This has been studied in probabilistic classification by [Buja et al. \(2005\)](#), and in the context of eliciting forecasts from experts by [Carvalho \(2016\)](#); [Merkle and Steyvers \(2013\)](#); [Bickel \(2007\)](#); [Machete \(2013\)](#). [Wheatcroft \(2021\)](#) articulated well the need for studying what forecasting errors different losses favor, and left it for future work. In the context of point forecasts, the same has been emphasized by [Ehm et al. \(2016\)](#) and [Patton \(2020\)](#). The work of [Machete \(2013\)](#) adopts a broadly similar approach to ours, though in a different setting, and reaches different conclusions. Recently, [Resin et al. \(2024\)](#) obtained a decomposition of the expected CRP loss into shift and dispersion components. Our work may be viewed as complementing theirs, toward an understanding of the behavior of CRP loss under differences in location and scale between the forecast and target distribution.

## 2 Preliminaries

We now introduce the formal setting which we study in this paper. Suppose that  $Y$  is a random variable taking values in an outcome space  $\mathcal{Y}$ , according to some probability distribution  $G$ . We call  $Y$  the *target variable* and  $G$  the *target distribution*. Letting  $\mathcal{F}$  denote a set of probability distributions on  $\mathcal{Y}$ , to measure how close a *forecast*  $F \in \mathcal{F}$  is to the target distribution, we define a *loss function*  $\ell : \mathcal{F} \times \mathcal{Y} \rightarrow [-\infty, \infty]$ , such that  $\ell(F, y)$  is the loss incurred for a forecast  $F$  of the observation  $y$ . The forecast  $F$  may be given in the form of a measure, density, cumulative distribution function, quantiles, or otherwise; different loss functions are defined in terms of different forms of inputs, in this regard. To keep the setting general and clear, we use the general word *distribution* to describe the forecast  $F$  and target  $G$  so as not to prefer any particular form. We assume that low *expected loss* indicates a good forecast, the expected loss defined as

$$\ell(F, G) = \mathbb{E}\ell(F, Y), \quad \text{for } Y \sim G.$$

(It will be clear from the context whether  $\ell$  denotes the loss or expected loss.) A loss is said to be *proper*, if

$$\ell(F, G) \geq \ell(G, G), \quad \text{for any } F, G.$$

In other words, if the target distribution itself minimizes the expected loss. A proper loss is said to be *strictly proper* if strict inequality holds in the above whenever  $F \neq G$ . Any proper loss induces a divergence

$$d(F, G) = \ell(F, G) - \ell(G, G),$$

which is nonnegative, and vanishes when the forecast  $F$  equals the target distribution  $G$ . We emphasize that in these definitions, and in our study in general, the forecast  $F$  is not treated as random, but as a fixed probability distribution.

### 2.1 Loss functions

We now introduce the loss functions studied in this paper. We refer the reader to [Gneiting and Raftery \(2007\)](#) for a more comprehensive review of loss functions in probabilistic forecasting.

**Logarithmic loss.** When the outcome space  $\mathcal{Y}$  is a convex subset of the finite-dimensional Euclidean space  $\mathbb{R}^d$ , and  $F, G$  are absolutely continuous with respect to the Lebesgue measure, we let  $f, g$  denote their respective densities. One of the earliest examples of proper losses, logarithmic loss ([Good, 1952](#)) is defined as the negative log-likelihood:

$$\ell(F, y) = -\log f(y).$$

Log loss is strictly proper if restricted to the family of densities with finite Shannon entropy (i.e.,  $\ell(F, F) < \infty$ ), and it induces the well-known Kullback–Leibler (KL) divergence ([Kullback and Leibler, 1951](#)):

$$d(F, G) = \int_{\mathcal{Y}} g(y) \log \frac{g(y)}{f(y)} dy = \mathbb{E} \left[ \log \frac{g(Y)}{f(Y)} \right] = \text{KL}(g||f),$$

recalling that  $Y$  is a random variable with distribution  $G$ . Logarithmic loss may be defined on a general outcome space  $\mathcal{Y}$ , given that  $F, G$  are both absolutely continuous with respect to a common measure on  $\mathcal{Y}$ , but the results in this paper pertain to Euclidean outcome spaces, as defined above. Log loss is commonly used in epidemiology (Reich et al., 2019) and in eliciting probabilities from experts (Carvalho, 2016).

**Quadratic loss.** In the same setting as logarithmic loss, quadratic loss (Brier, 1950) is affine in the likelihood:

$$\ell(F, y) = -2f(y) + \int_{\mathcal{Y}} f(x)^2 dx,$$

assuming the density  $f$  is square integrable. The integral term constitutes a penalty for low entropy. Quadratic loss is strictly proper. It is worth noting that if the integral penalty is omitted, then the loss becomes improper. The induced divergence is the squared  $L^2$  distance between the densities:

$$d(F, G) = \int_{\mathcal{Y}} (f(y) - g(y))^2 dy.$$

Quadratic loss is sometimes used in the setting of forecast aggregation (Hora and Kardes, 2015). More recently, it has been used to evaluate estimated distributions of network traffic features (Dietmüller et al., 2024).

**Spherical loss.** In the same setting as quadratic losses, spherical loss (Roby, 1965) is now linear in the likelihood:

$$\ell(F, y) = -f(y) \left( \int_{\mathcal{Y}} f(x)^2 dx \right)^{-\frac{1}{2}},$$

assuming the density is square integrable. Similar to quadratic loss, the integral term here constitutes a penalty for low entropy. Spherical loss is strictly proper, and the induced divergence is

$$d(F, G) = \left( \int_{\mathcal{Y}} g(y)^2 dy \right)^{\frac{1}{2}} - \left( \int_{\mathcal{Y}} f(y)^2 dy \right)^{-\frac{1}{2}} \int_{\mathcal{Y}} f(y)g(y) dy.$$

Spherical loss is a special case of pseudospherical loss (Good, 1971). This has recently gained popularity in machine learning, with Yu et al. (2021) deriving an efficient approach for fitting for energy-based models via minimization of pseudospherical loss functions. Lee and Lee (2022) proposed using a pseudospherical loss in knowledge distillation, whose goal is to transfer knowledge from a larger to a smaller model.

**Continuous ranked probability (CRP) loss.** Unlike logarithmic, quadratic, and spherical losses, we now no longer require the existence of densities. In the case that the outcome space  $\mathcal{Y}$  is a convex subset of the real line  $\mathbb{R}$ , we identify  $F$  with a cumulative distribution function. Continuous ranked probability (CRP) loss (Matheson and Winkler, 1976) is defined by

$$\ell(F, y) = \int_{\mathcal{Y}} (F(x) - \mathbb{I}\{y \leq x\})^2 dx.$$

where  $\mathbb{I}\{y \leq x\}$  is equal to 1 if  $y \leq x$  and 0 otherwise. This has the alternative representation (Baringhaus and Franz, 2004; Székely and Rizzo, 2005):

$$\ell(F, y) = \mathbb{E}|X - X'| \left( \frac{\mathbb{E}|X - y|}{\mathbb{E}|X - X'|} - \frac{1}{2} \right),$$

where  $X, X' \sim F$  are independent. The multiplier  $\mathbb{E}|X - X'|$  outside of the parentheses serves as a penalty for high entropy (in contrast to quadratic and spherical losses), as the term inside the parentheses is scale invariant. CRP loss is strictly proper if restricted to the family of distributions with finite first moment. It induces the Cramér divergence (Cramér, 1928):

$$d(F, G) = \int_{\mathcal{Y}} (F(y) - G(y))^2 dy.$$

These properties of CRP loss—that it does not require a forecast to have a density, and has a representation in terms of expectations—make it quite popular. In particular, CRP loss is widely used in atmospheric sciences (Gneiting et al., 2005; Scheuerer and Möller, 2015; Rasp and Lerch, 2018; Kochkov et al., 2024; Clement and Zaoui, 2024), and features

in isotonic distributional regression (Henzi et al., 2021). In addition, CRP loss has another alternative representation as an integrated loss in terms of the quantile function  $F^{-1}$  (Laio and Tamea, 2007). This provides a close connection to (weighted) interval score, which has recently become popular in epidemic forecasting (Bracher et al., 2021).

**Threshold-weighted CRP loss.** A threshold-weighted version of CRP loss (Matheson and Winkler, 1976; Gneiting and Ranjan, 2011) generalizes CRP loss by introducing a nonnegative integrable weight function  $w : \mathcal{Y} \rightarrow [0, \infty)$ , via

$$\ell(F, y) = \int_{\mathcal{Y}} w(x)(F(x) - \mathbb{I}\{y \geq x\})^2 dx.$$

This has the alternative representation in terms of expectations:

$$\ell(F, y) = \mathbb{E}|v(X) - v(X')|\left(\frac{\mathbb{E}|v(X) - v(y)|}{\mathbb{E}|v(X) - v(X')|} - \frac{1}{2}\right),$$

where  $X, X' \sim F$  are independent, and where  $v$  is any antiderivative of  $w$  (i.e.,  $v' = w$ ). Threshold-weighted CRP loss is strictly proper if restricted to the family of distributions with finite first moment, and restricted to a strictly positive weight function. It induces the weighted Cramér divergence:

$$d(F, G) = \int_{\mathcal{Y}} w(y)(F(y) - G(y))^2 dy.$$

Threshold-weighted CRP loss is used in the forecasting of high-impact events, for example, in meteorological sciences (Allen et al., 2023a; Taillardat et al., 2023). We refer to the case where the weight function is a power,  $w(y) = y^\alpha$  for  $\alpha \in \mathbb{R}$ , as a power-weighted CRP loss.

**Energy loss.** Generalizing CRP in a different direction is the energy loss (Gneiting and Raftery, 2007), which extends the expectation formulation of CRP to a multidimensional outcome space  $\mathcal{Y} \subseteq \mathbb{R}^d$ , using a parameter  $\beta \in (0, 2)$ , via

$$\ell(F, y) = \mathbb{E}\|X - X'\|_2^\beta \left(\frac{\mathbb{E}\|X - y\|_2^\beta}{\mathbb{E}\|X - X'\|_2^\beta} - \frac{1}{2}\right),$$

where  $X, X' \sim F$  are independent, and  $\|\cdot\|_2$  denotes the Euclidean norm. Note that CRP loss is given by the special case where  $d = \beta = 1$ . As with CRP loss, the multiplier outside of the parentheses may be seen as a penalty for high entropy. Energy loss is strictly proper if restricted to the family of distributions with finite  $\beta$ -moment. The induced divergence is the generalized energy distance:

$$d(F, G) = \mathbb{E}\|X - Y\|_2^\beta - \frac{1}{2}\left(\mathbb{E}\|X - X'\|_2^\beta + \mathbb{E}\|Y - Y'\|_2^\beta\right),$$

which is related to energy statistics (Székely and Rizzo, 2013). Here,  $X, X', Y, Y'$  are independent random variables having distributions  $F, F, G, G$ , respectively. As a generalization of CRP loss, energy loss is employed in many of the same application areas and also admits weighted versions that are used to evaluate, for example, forecasts of extreme meteorological events (Allen et al., 2023b).

**Dawid–Sebastiani (DS) loss.** Introduced in Dawid and Sebastiani (1999) originally for non-forecasting purposes, the Dawid–Sebastiani (DS) loss is given for a real-valued outcome space  $\mathcal{Y} \subseteq \mathbb{R}$  by

$$\ell(F, y) = \log \text{Var}(X) + \frac{(y - \mathbb{E}X)^2}{\text{Var}(X)},$$

where  $X \sim F$ , assumed to have finite variance. It is, up to additive and multiplicative constants, the logarithmic loss when the input is normally distributed with the same mean and variance as the forecast  $F$ . Being dependent only on the forecast mean and variance, it is proper but not strictly proper. The induced divergence is

$$d(F, G) = \log \frac{\text{Var}(X)}{\text{Var}(Y)} + \frac{\text{Var}(Y) - \text{Var}(X) + (\mathbb{E}Y - \mathbb{E}X)^2}{\text{Var}(X)},$$

where recall  $Y \sim G$ . This identifies with the divergence induced by logarithmic loss when both the forecast and target distributions are normal, with mean and variance equal to those of  $F$  and  $G$ , respectively. DS loss (or its multivariate extension) have been used as approximations to logarithmic and energy losses, in meteorology (Feldmann et al., 2015; Scheurer and Hamill, 2015), epidemiology (Meyer and Held, 2014) and economics (Lerch et al., 2017).

## 2.2 More background and commentary

A loss  $\ell$  is said to be *local* if  $\ell(F, y)$  depends only on the observed target  $y$ , and the density evaluated at the target  $f(y)$ . Up to affine transformations, logarithmic loss is the only proper loss that is local, for outcome spaces with more than two elements (Bernardo, 1979; Parry et al., 2012). Some authors argue that locality is a desirable property on philosophical grounds—a local loss depends only on target values that were realized. On the other hand, proper losses that naturally derive from decision making tasks are often non-local (Dawid, 2007). In some situations, it can be demanding or even intractable to compute a function of the entire distribution. Indeed, Shao et al. (2024) state that in language modeling the logarithmic loss is almost exclusively used, due in part to its desirable characteristics and in part to its tractability given the notoriously large sample space.

The log loss can be infinite if the forecast fails to attribute positive density to the observed outcome. Proponents of this property argue it elicits careful assessment of all possible events, no matter how unlikely they are (Benedetti, 2010), while opponents point to the difficulty and potential arbitrariness in assigning very small probabilities simply to avoid an infinite loss (Selten, 1998).

In weather and climate applications, it is common to form a probabilistic ensemble forecast out of point predictions from numerical simulation models with different initial conditions (Leutbecher and Palmer, 2008). CRP loss is widespread in those fields, with extensive use that can be partially explained by the convenience it provides: when CRP is represented in its alternative expectation-based form, the forecast  $F$  can be readily replaced by sample averages over the members of an ensemble, or the output of a Markov chain Monte Carlo procedure (Gneiting et al., 2007; Allen et al., 2023a). Compared to the logarithmic loss, a further reason for using CRP is that it retains propriety when straightforward and natural weighting schemes are applied to emphasize certain events (Matheson and Winkler, 1976; Gneiting and Ranjan, 2011), whereas the logarithmic loss does not (Amisano and Giacomini, 2007), and weighting schemes that maintain propriety for log loss can be less intuitive.

## 3 Main results

We now turn to proving the main results, dividing our presentation on scale families (Section 3.1), location families (Section 3.2), and exponential families (Section 3.3).

### 3.1 Scale families

For a scale family  $\{G_\sigma : \sigma > 0\}$ , in order to study asymmetry inherent to a loss  $\ell$  (whether  $\ell$  favors overestimating or underestimating the scale  $\sigma$ ), we impose two conditions on the associated divergence  $d$ . First we assume  $d$  is *symmetric*, which means it is invariant to the order of its arguments, that is,

$$d(F, G) = d(G, F), \quad \text{for all } F, G.$$

It is clear from their definitions in Section 2 that the divergences induced by quadratic, CRP, threshold-weighted CRP, and energy losses are symmetric, whereas those induced by spherical, DS, and logarithmic losses are not. Spherical and DS losses deviate from symmetry in ways that Theorem 1—proved in this subsection—is able to accommodate, while logarithmic loss does not and is left for later treatment.

The second requirement is that there exists a function  $h : (0, \infty) \rightarrow (0, \infty)$  such that

$$d(F_\sigma, G_\tau) = h(\tau)d(F_{\sigma/\tau}, G_1), \quad \text{for all } \sigma, \tau > 0,$$

and for all scale families  $\{F_\sigma : \sigma > 0\}, \{G_\sigma : \sigma > 0\}$ . This says that the forecast and target distributions can be jointly rescaled by the same factor, at the cost of a multiplicative element applied to the divergence. We call divergences which satisfy this condition *rescalable*, and we call  $h$  the *scaling* function. Note that  $h$  must always satisfy  $h(1) = 1$ .

Interestingly, the only possible continuous scaling functions  $h$  are real powers:  $h(\sigma) = \sigma^\gamma$ , for some  $\gamma \in \mathbb{R}$ . Indeed, if we equate rescaling by  $\sigma\tau$  to rescaling by  $\sigma$  and then  $\tau$ , we obtain the identity  $h(\sigma\tau) = h(\sigma)h(\tau)$ , for  $\sigma, \tau > 0$ . This is often called Pexider's equation, and subject to  $h(1) = 1$ , the only continuous functions which satisfy this equation are real powers (Small, 2007).

The following lemma summarizes the rescalability properties of the loss functions discussed in this paper.

**Lemma 1.** *The following holds.*

- CRP loss induces a rescalable divergence, with  $h(\sigma) = \sigma$ .
- Energy loss induces a rescalable divergence, with  $h(\sigma) = \sigma^\beta$ .
- Quadratic loss induces a rescalable divergence, with  $h(\sigma) = 1/\sigma$ .
- Logarithmic and DS losses induce rescalable divergences, with  $h(\sigma) = 1$ .
- Power-weighted CRP loss ( $w(y) = y^\alpha$ ) induces a rescalable divergence, with  $h(\sigma) = \sigma^{\alpha+1}$ .

The proof in each case is by change of variables and is omitted.

From the perspective of Theorem 1, what shall matter is whether the scaling  $h$  is an increasing, decreasing or constant function. To be clear, we say that  $h$  is increasing if  $h(x) < h(y)$  for all  $0 < x < y$ , and decreasing if  $-h$  is increasing. The divergences induced by CRP, energy, and power-weighted CRP (with  $\alpha > -1$ ) losses have an increasing scaling function, and the ones induced by quadratic and power-weighted CRP (with  $\alpha < -1$ ) losses have a decreasing scaling function. The divergences induced by DS, logarithmic and power-weighted CRP (when  $\alpha = -1$ ) losses have constant scaling, so we may call them *scale invariant*.

A key step for the proof of Theorem 1 is given in the next lemma, which characterizes whether a loss function favors underestimating the scale, overestimating it, or neither, based on symmetry and rescalability of the induced divergence.

**Lemma 2.** *Let  $\{G_\sigma : \sigma > 0\}$  be a scale family,  $\ell$  a loss function, and  $d$  the induced divergence. If  $d$  is symmetric and rescalable with scaling function  $h$ , then the following holds for  $G = G_1$  and all  $\sigma > 1$ .*

- If  $h$  is increasing, then  $\ell(G_\sigma, G) > \ell(G_{1/\sigma}, G)$ .
- If  $h$  is decreasing, then  $\ell(G_\sigma, G) < \ell(G_{1/\sigma}, G)$ .
- If  $h$  is constant, then  $\ell(G_\sigma, G) = \ell(G_{1/\sigma}, G)$ .

*Proof.* Using symmetry then rescalability, we compute:

$$d(G_\sigma, G) = d(G, G_\sigma) = h(\sigma)d(G_{1/\sigma}, G).$$

Suppose that the scaling  $h$  is increasing, so that  $h(\sigma) > h(1) = 1$ . It follows that  $d(G_\sigma, G) > d(G_{1/\sigma}, G)$ , from which we conclude  $\ell(G_\sigma, G) - \ell(G_{1/\sigma}, G) = d(G_\sigma, G) - d(G_{1/\sigma}, G) > 0$ . The cases where the scaling  $h$  is decreasing or constant follow similarly.  $\square$

The proof of Theorem 1 is now just a matter of putting together Lemmas 1 and 2, with some additional work along the same lines to accommodate spherical and DS losses.

*Proof of Theorem 1.* CRP and energy losses are symmetric and by Lemma 1 they are rescalable with increasing scaling. Hence Lemma 2 implies  $\ell(G_\sigma, G) > \ell(G_{1/\sigma}, G)$  as required. Meanwhile, quadratic loss is symmetric and by Lemma 1 it is rescalable with decreasing scaling, so by Lemma 2 we conclude that  $\ell(G_\sigma, G) < \ell(G_{1/\sigma}, G)$ , as required.

Suppose now that  $\ell$  is the spherical loss. The induced divergence  $d$  is neither symmetric nor rescalable. However, when the forecast and target distribution are members of the same scale family, we have the following two properties. First, a condition similar to rescalability holds, with decreasing scaling:

$$d(G_\sigma, G_\tau) = \frac{1}{\sqrt{\tau}}d(G_{\sigma/\tau}, G).$$

This may be shown using a change of variables. Second, a property related to symmetry holds:

$$d(G_\sigma, G_\tau) = \sqrt{\frac{\sigma}{\tau}}d(G_\tau, G_\sigma).$$

Interestingly, the effects of the two multiplicative factors above cancel each other, resulting in  $d(G_\sigma, G) = \sqrt{\sigma}d(G, G_\sigma) = d(G_{1/\sigma}, G)$ , and thus  $\ell(G_\sigma, G) = \ell(G_{1/\sigma}, G)$ , as required.

Finally, for  $\ell$  being DS loss, and  $d$  the associated divergence, we may check by direct differentiation that

$$d(G_{1/\sigma}, G) - d(G_\sigma, G) = \left( \sigma^2 - \frac{1}{\sigma^2} \right) - 2 \log \sigma > 0.$$

Consequently,  $\ell(G_\sigma, G) < \ell(G_{1/\sigma}, G)$ , as required. This completes the proof.  $\square$

### 3.2 Location families

The argument for a location family  $\{G_\mu : \mu \in \mathbb{R}\}$  is broadly similar to that given in the previous subsection for a scale family. We assume that the divergence  $d$  induced by the given loss  $\ell$  is symmetric as well as *translation invariant*:

$$d(F_\mu, G_\nu) = d(F_{\mu-\nu}, G_0), \quad \text{for all } \mu, \nu \in \mathbb{R},$$

and for all location families  $\{F_\mu : \mu \in \mathbb{R}\}, \{G_\mu : \mu \in \mathbb{R}\}$ . It is clear from their definitions in Section 2 that the divergences induced by quadratic, CRP, energy, spherical, DS, and logarithmic losses are translation invariant.

The next lemma is similar to Lemma 2 and is key to the proof of Theorem 3.

**Lemma 3.** *Let  $\{G_\mu : \mu \in \mathbb{R}\}$  be a location family,  $\ell$  a loss function, and  $d$  the induced divergence. If  $d$  is symmetric and translation invariant, then  $\ell(G_\mu, G) = \ell(G_{-\mu}, G)$  for  $G = G_0$  and all  $\mu \in \mathbb{R}$ .*

*Proof.* Using symmetry then translation invariance,  $d(G_\mu, G) = d(G, G_\mu) = d(G_{-\mu}, G)$ . We conclude  $\ell(G_\mu, G) - \ell(G_{-\mu}, G) = d(G_\mu, G) - d(G_{-\mu}, G) = 0$ .  $\square$

We now prove Theorem 3.

*Proof of Theorem 3.* For quadratic, CRP, and energy losses, the associated divergences are symmetric and translation invariant, so application of Lemma 3 leads to the desired results.

The divergences induced by spherical and DS losses are translation invariant, and furthermore they are symmetric when restricted to the case where the forecast and target distribution both belong to the same location family. Therefore the same argument as in Lemma 3 gives the desired result for spherical and DS losses.

For logarithmic loss, let  $g$  be the Lebesgue density of  $G$ . Recall  $g$  is itself assumed to be symmetric, and by translation invariance we may assume, without loss of generality, that  $g$  is symmetric around zero, i.e.,  $g(y) = g(-y)$ . By a change of variables, followed by symmetry,

$$d(G_\mu, G) = \int g(y) \log \frac{g(y)}{g(y-\mu)} dy = \int g(-y) \log \frac{g(-y)}{g(-y-\mu)} dy = \int g(y) \log \frac{g(y)}{g(y+\mu)} dy = d(G_{-\mu}, G).$$

We conclude that  $\ell(G_\mu, G) = \ell(G_{-\mu}, G)$ , as required.  $\square$

### 3.3 Exponential families

For logarithmic loss, the arguments given in Section 3.1, which are based on symmetry of the divergence, do not apply. Indeed, the KL divergence, which is the divergence associated with log loss and is not symmetric in its arguments, can behave in subtle ways for scale families. For the Cauchy scale family, log loss is actually symmetric in its penalty for  $\sigma$  versus  $1/\sigma$  (this follows from Nielsen, 2019), which shows that this loss does not always favor overestimating a scale parameter, despite what the empirical results in Figures 1 and 2 might seem to suggest at face value.

The approach we take in this subsection is to characterize the asymmetries inherent to logarithmic loss within minimal single-parameter exponential families. Let  $\{p_\eta : \eta > 0\}$  be a minimal exponential family of densities, where

$$p_\eta(x) = h(x) e^{\eta T(x) - A(\eta)},$$

and the sufficient statistic  $T$  is not almost everywhere constant. Below we establish conditions for the logarithmic loss to favor forecasting  $p_{\theta\eta}$  over  $p_{\eta/\theta}$ , the opposite, or neither, for any  $\theta > 1$ , when the target distribution is  $p_\eta$ . These

conditions are described in terms of the second derivative of the log-partition function  $A(\eta)$ ; note the second derivative always exists and is nonnegative (Keener, 2010). In particular, logarithmic loss will favor underestimating the natural parameter if the acceleration  $A''(\eta)$  dominates a rate  $1/\eta^3$ , in a particular sense to be made precise. On the other hand, logarithmic loss will favor overestimating the natural parameter for exponential families where the acceleration  $A''(\eta)$  is dominated by the rate  $1/\eta^3$ . When the natural parameter space is the entire real line (instead of the positive reals), we derive similar conditions defined in terms of  $A''(\eta)$  versus  $A''(-\eta)$ . Our results are summarized in the following.

**Lemma 4.** *Let  $\{p_\eta : \eta \in \Omega\}$  be a minimal single-parameter exponential family, with the log-partition function  $A(\eta)$ . Denote by  $\ell$  the logarithmic loss. If  $\Omega = (0, \infty)$ , then the following holds for all  $\eta \in \Omega$  and all  $\theta > 1$ .*

1. If  $u^3 A''(u)$  is increasing in  $u$ , then  $\ell(p_{\theta\eta}, p_\eta) > \ell(p_{\eta/\theta}, p_\eta)$ .
2. If  $u^3 A''(u)$  is decreasing in  $u$ , then  $\ell(p_{\theta\eta}, p_\eta) < \ell(p_{\eta/\theta}, p_\eta)$ .
3. If  $u^3 A''(u)$  is constant in  $u$ , then  $\ell(p_{\theta\eta}, p_\eta) = \ell(p_{\eta/\theta}, p_\eta)$ .

If  $\Omega = \mathbb{R}$ , then the following holds for all  $\eta \in \Omega$  and all  $\theta > 0$ .

1. If  $A''(u) - A''(-u)$  is increasing in  $u$ , then  $\ell(p_{\eta+\theta}, p_\eta) > \ell(p_{\eta-\theta}, p_\eta)$ .
2. If  $A''(u) - A''(-u)$  is decreasing in  $u$ , then  $\ell(p_{\eta+\theta}, p_\eta) < \ell(p_{\eta-\theta}, p_\eta)$ .
3. If  $A''(u) - A''(-u)$  is constant in  $u$ , then  $\ell(p_{\eta+\theta}, p_\eta) = \ell(p_{\eta-\theta}, p_\eta)$ .

*Proof.* Suppose  $\Omega = (0, \infty)$ . Using scale invariance, we may assume without loss of generality that  $\eta = 1$ . Denoting  $p = p_1$ , note that the difference in divergence can be written as

$$\ell(p_\theta, p) - \ell(p_{1/\theta}, p) = d(p_\theta, p) - d(p_{1/\theta}, p) = \mathbb{E} \log \frac{p_{1/\theta}(Y)}{p_\theta(Y)} = A(\theta) - A(1/\theta) - (\theta - 1/\theta) \mathbb{E} T(Y),$$

where recall  $Y$  is a random variable with density  $p$ . A standard exponential family identity states that  $\mathbb{E} T(Y) = A'(1)$ , hence we may write

$$\ell(p_\theta, p) - \ell(p_{1/\theta}, p) = d_A(\theta, 1) - d_A(1/\theta, 1),$$

where  $d_A(y, x) = A(y) - A(x) - A'(x)(y - x)$  is the Bregman divergence associated with the log-partition function  $A$ . Assume  $u^3 A''(u)$  is increasing. Applying the fundamental theorem of calculus twice, we bound one of the Bregman divergences from below,

$$d_A(\theta, 1) = \int_1^\theta \int_1^v A''(u) dudv = \int_1^\theta \int_1^v \frac{u^3 A''(u)}{u^3} dudv > A''(1) \int_1^\theta \int_1^v \frac{dudv}{u^3}.$$

Applying the same argument again, we bound the other Bregman divergence from above,

$$d_A(1/\theta, 1) = \int_{1/\theta}^1 \int_v^1 A''(u) dudv = \int_{1/\theta}^1 \int_v^1 \frac{u^3 A''(u)}{u^3} dudv < A''(1) \int_{1/\theta}^1 \int_v^1 \frac{dudv}{u^3}.$$

Now, the statement  $\ell(p_\theta, p) > \ell(p_{1/\theta}, p)$  will have been established as soon as we notice that the two integrals identify,

$$\int_1^\theta \int_1^v \frac{dudv}{u^3} = \frac{(\theta - 1)^2}{2\theta} = \int_{1/\theta}^1 \int_v^1 \frac{dudv}{u^3}.$$

The statements for  $u^3 A''(u)$  decreasing and constant, as well as the statements for the case that  $\Omega = \mathbb{R}$ , are proven in a similar way, and we omit the details.  $\square$

We now turn to proving Theorem 2. Before we do that, let us define the exponential families covered by the theorem.

- The generalized gamma scale family has density  $g_\sigma(x) = \Gamma(k/\gamma)^{-1} \sigma^{-k} \gamma x^{k-1} e^{-(x/\sigma)^\gamma}$ , for  $x, \sigma, \gamma, k > 0$ , and where  $\Gamma$  is the gamma function. Here the natural parameter is  $\eta = \sigma^{-\gamma} \in (0, \infty)$  and the log-partition function is  $A(\eta) = -(k/\gamma) \log \eta$ . Special cases are the gamma scale family ( $\gamma = 1$ ), exponential scale family ( $\gamma = 1$  and  $k = 1$ ) and the Weibull scale family ( $k = \gamma$ ). If the generalized gamma scale family is extended by symmetry to  $x \in \mathbb{R}$ , we obtain the Laplace scale family ( $\gamma = 1$  and  $k = 1$ ) and the normal scale family ( $\gamma = 2$  and  $k = 1$ ).

- The log-normal log-scale family has density  $g_\sigma(x) = (x\sigma\sqrt{2\pi})^{-1}e^{-(\log x - \mu)^2/(2\sigma^2)}$ , where  $x, \sigma > 0$  and  $\mu \in \mathbb{R}$ . The natural parameter is  $\eta = \sigma^{-2} \in (0, \infty)$  and the log-partition function is  $A(\eta) = -(1/2)\log\eta$ .
- The inverse gamma scale family has density  $g_\sigma(x) = \Gamma(k)^{-1}\sigma^k x^{-k-1}e^{-\sigma/x}$ , for  $x, \sigma, k > 0$ . Here the natural parameter is  $\eta = \sigma \in (0, \infty)$  and the log-partition function is  $A(\eta) = -k\log\eta$ .
- The generalized gamma shape family has density  $g_k(x) = \Gamma(k/\gamma)^{-1}\sigma^{-k}\gamma x^{k-1}e^{-(x/\sigma)^\gamma}$ , for  $x, \sigma, \gamma, k > 0$ . The natural parameter is  $\eta = k \in (0, \infty)$  and the log-partition function is  $A(\eta) = (\log\sigma)\eta + \log\Gamma(\eta/\gamma)$ . A special case is the gamma shape family ( $\gamma = 1$ ).
- The Pareto shape family has density  $g_k(x) = km^k/x^k$ , for  $x \geq m$  and  $k, m > 0$ . Here the natural parameter is  $\eta = k \in (0, \infty)$  and the log-partition function is  $A(\eta) = -\log\eta - (\log m)\eta$ .
- The inverse Gaussian shape family has density  $g_k(x) = \sqrt{k/2\pi x^3}e^{-k(x-\mu)^2/(2\mu^2x)}$ , for  $x, k, \mu > 0$ . The natural parameter is  $\eta = k \in (0, \infty)$  and the log-partition function is  $A(\eta) = -(1/2)\log\eta$ .
- The beta shape family has density  $g_k(x) = x^{k-1}(1-x)^{\beta-1}\Gamma(k+\beta)/(\Gamma(k)\Gamma(\beta))$ , for  $x \in [0, 1]$  and  $k, \beta > 0$ . The natural parameter is  $\eta = k \in (0, \infty)$  and the log-partition function is  $A(\eta) = -\log(\Gamma(\eta+\beta)/\Gamma(\eta))$ .
- The Poisson rate family has density  $g_\lambda(k) = \lambda^k e^{-\lambda}/k!$ , for  $k \geq 0$  integer and  $\lambda > 0$ . Here the natural parameter is  $\eta = \log\lambda \in \mathbb{R}$  and the log-partition function is  $A(\eta) = e^\eta$ .

*Proof of Theorem 2.* For families with a log-partition function of the form  $A(\eta) = -a\log\eta + b\eta$ , where  $a > 0$  and  $b \in \mathbb{R}$ , the acceleration is  $A''(\eta) = a/\eta^2$  which means that  $u^3 A''(u)$  is increasing in  $u$ . Hence, by Lemma 4, we have  $\ell(p_{\theta\eta}, p_\eta) > \ell(p_{\eta/\theta}, p_\eta)$  for all  $\eta > 0$  and all  $\theta > 1$ . Consequently, for the generalized gamma scale family, as the scale parameter  $\sigma$  is inversely proportional to the natural parameter  $\eta = 1/\sigma^\gamma$ , we have, writing  $g_{\theta^{1/\gamma}}$  for the density of  $G_\theta$ ,

$$\ell(G_{1/\theta}, G) = \ell(g_{\theta^{-1/\gamma}}, g) = \ell(p_\theta, p) > \ell(p_{1/\theta}, p) = \ell(g_{\theta^{1/\gamma}}, g) = \ell(G_\theta, G),$$

for all  $\theta > 1$ . As special cases, we obtain the required results for gamma, exponential and Weibull scale families. By symmetrization, the same applies to the Laplace and normal scale families as well, and analogous arguments hold for log-normal log-scale family, inverse gamma scale family, and the Pareto and inverse Gaussian shape families.

For the generalized gamma shape family, the acceleration is  $A''(\eta) = \gamma^{-2}\psi'(\eta/\gamma)$ , where  $\psi$  is the digamma function. It suffices to show that  $f(x) = x^3\psi'(x)$  is an increasing function of  $x$ . From the series representation (Arfken et al., 2011)

$$\psi'(x) = \sum_{n=0}^{\infty} \frac{1}{(x+n)^2} \quad \text{and} \quad \psi''(x) = -\sum_{n=0}^{\infty} \frac{2}{(x+n)^3},$$

valid for all  $x > 0$ , we differentiate:

$$f'(x) = 3x^2\psi'(x) + x^3\psi''(x) = x^2 \sum_{n=0}^{\infty} \frac{x+3n}{(x+n)^3} > 0.$$

Therefore,  $f$  is increasing, consequently  $u^3 A''(u)$  is increasing in  $u$ , and by Lemma 4 we obtain the desired result. As a special case we obtain the desired result for the gamma shape family. For the beta shape family, the acceleration is  $A''(\eta) = \psi'(\eta) - \psi'(\eta+\beta)$ , and it suffices to show that  $f(x) = x^3(\psi'(x) - \psi'(x+\beta))$  is an increasing function of  $x$ . We use the series representation to differentiate:

$$f'(x) = (3x^2\psi'(x) + x^3\psi''(x)) - (3x^2\psi'(x+\beta) + x^3\psi''(x+\beta)) = x^2 \sum_{n=0}^{\infty} \left( \frac{x+3n}{(x+n)^3} - \frac{x+3(\beta+n)}{(x+\beta+n)^3} \right).$$

As  $a \mapsto (x+3a)/(x+a)^3$  is decreasing, the derivative  $f'$  is positive, thus  $f$  is increasing. Consequently,  $u^3 A''(u)$  is increasing in  $u$ , and by Lemma 4 we obtain the desired result. Finally, for the Poisson rate family, the acceleration is  $A''(\eta) = e^\eta$ , with  $\Omega = \mathbb{R}$ . Since  $A''$  is increasing, by Lemma 4 we obtain the desired result, completing the proof.  $\square$

**Remark 1.** Using the same approach, we may obtain similar results for further exponential families, and we omit the details. Examples of such families to which this method is applicable: normal location family, log-normal log-location family, inverse Gaussian mean family, binomial family with success probability as parameter.

## 4 Empirical results

We now discuss in greater detail the experiments presented in the introduction, and report further results. We begin by highlighting the implications of the asymmetries underlying proper loss functions on real data, over three domains. A comprehensive synthetic experiment across five proper loss functions finishes this section, which corroborates many of our previous findings and motivates directions for future work. All of our results are reproducible from the code available at <https://github.com/jv-rv/loss-asymmetries/>.

### 4.1 Covid-19 mortality

The Covid-19 Forecast Hub (Cramer et al., 2022a) has been used by the U.S. Centers for Disease Control and Prevention (CDC) to communicate information leading to policy decisions, including as to the allocation of ventilators, vaccines, and medical staff across geographic locations over the Covid-19 pandemic. We restrict our attention to death forecasts, as in Cramer et al. (2022b), and we analyze weekly predictions from dozens of forecasters of the number of Covid-19 deaths one through four weeks ahead, for each U.S. state, over the period from April 2020 to March 2023. All forecasts in the Hub are stored in quantile format, and so we converted each forecast from a discrete set of quantiles to a density or CDF before compute log or CRP loss, respectively. Details are given in Appendix A.1.

To compute the heatmap in Figure 2, we applied transformations to the forecasts and the target data, as follows. First, we estimated and applied nonparametric transformations to standardize the target distribution, giving it approximately mean zero and variance one at every time point and for every location; details are given in Appendix A.2. Second, we centered and scaled each input forecast distribution in the Covid-19 Hub, giving it mean  $\mu$  and variance  $\sigma$ , and then we evaluated the loss (logarithmic or CRP) between the transformed forecast distribution and standardized target value. We averaged these loss values over all dates, all locations, and all forecasters; this was done over a fine grid of  $\mu, \sigma$  values in order to create the heatmap (each pair  $\mu, \sigma$  corresponds to a particular pixel value). Lastly, the color scale for the losses in Figures 1 and 2 (as well as Figure 6) was set nonlinearly in order to better emphasize the sublevel sets.

Figure 3 reports the standardized ranking of ten forecasters who participated in the Covid-19 Forecast Hub and received the top scores in Figure 2 of Cramer et al. (2022b). The standardized ranking is computed in the same manner as that paper, as follows. For each state, date and weeks ahead, we ranked the forecasters according to loss, then divided by the number of forecasters which submitted a forecast for the state-date-weeks-ahead combination. This is the standardized ranking value, between zero and one, which we then averaged for each forecaster across states, dates, and weeks ahead. Each column of Figure 3 displays this for a different choice of loss—log loss (left column) and CRP loss (right). To further annotate, we identified the four forecasters with the highest standardized ranking according to forecast variance (instead of loss) and the four lowest. For the four with the highest standardized variance, logarithmic loss ranked each one at least as high as CRP loss, with an average margin of 2 places. For the four with the lowest standardized variance, CRP loss ranked each one at least as high as log loss, with an average margin of 1.75 places.

### 4.2 Retail sales

The Makridakis Competitions are well-known in the applied forecasting community, with the initial edition beginning over 40 years ago (Makridakis et al., 1982). The fifth edition introduced an uncertainty track called the M5 Uncertainty Competition (Makridakis et al., 2022), in which teams were tasked with forecasting nine quantiles of future retail sales for a myriad of products, aggregation levels, and horizons. Out of almost 900 competing teams, the 50 with best average performance, according to a weighted and scaled version of the quantile loss, had their forecasts published. Demand is notoriously intermittent, especially at the least aggregated level, which posed a steep challenge to forecasters. Many of the best-performing teams used gradient boosting (Friedman, 2001) to predict quantiles. As we did with the forecasts in the Covid-19 Forecast Hub, we converted these quantile forecasts into a density or CDF before computing log or CRP loss, respectively, following the same strategy as that outlined in Appendix A.1.

Each forecaster was then ranked among all forecasts issued for each prediction task, and the rankings were standardized to be between zero and one. Averaging the standardized ranks coming from logarithmic and CRP losses, as we did in the Covid-19 experiment, yielded Figure 4 in the introduction. As we can see, log loss clearly prefers the forecasters that have higher standardized forecast variance (from left to right, there is clear downward movement in the rankings of highest-variance forecasters), while CRP clearly prefers the opposite (from left to right, clear upward movement in the rankings of lowest-variance forecasters).

### 4.3 Temperature extremes

The Coupled Model Intercomparison Project (CMIP) is a significant project collecting the results of climate simulation models, introduced nearly 30 years ago by Meehl et al. (1997). Here we consider the maximum temperatures over the boreal summer simulated by the 30 models available from its sixth edition CMIP6 (Eyring et al., 2016). We source the target data from Hadex3 (Dunn et al., 2020), a data set of monthly extreme temperatures (and other climate data) on a spatial grid, based on observations recorded from thousands of meteorological stations across the world.

Using historical runs of each model from 1950 to 2014, we first calculated the predicted monthly maximum temperature from the available daily data. We then translated each model’s simulated predictions to Hadex3’s spatial grid via bilinear interpolation routines from the Climate Data Operators collection (Schulzweida, 2023). After this step, each model has 195 simulated maximum temperatures at 3055 spatial locations (grid points). Adopting a similar approach to previous work in the literature (Thorarinsdottir et al., 2020), we applied kernel density estimation—with a Gaussian kernel and Scott’s rule for automatic bandwidth selection (Scott, 1992)—in order to form a forecast distribution at each location. The same was done with the target data, in order to form a target distribution at each location. (We ensure densities at each location have the same support fitting exponential tails to the extreme samples.)

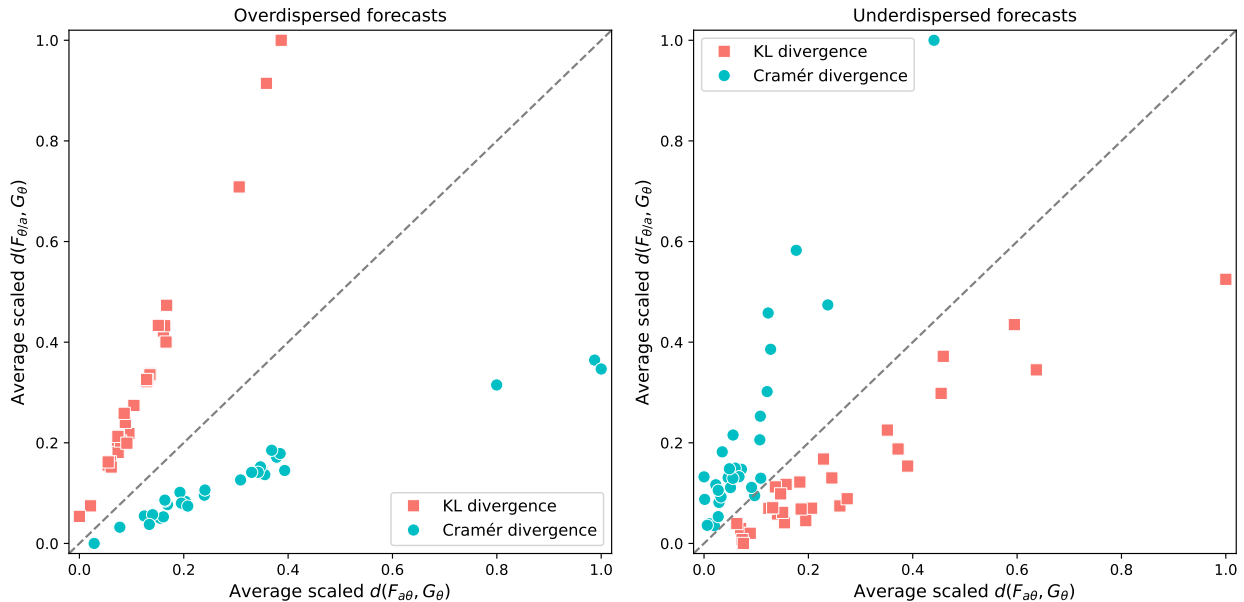


Figure 5: Average divergence for 30 models in CMIP6, in cases where they are initially overdispersed (left panel) or underdispersed (right panel). For each forecast distribution  $F_{a\theta}$ , and target distribution  $G_\theta$ , we compare divergences  $d(F_{a\theta}, G_\theta)$  and  $d(F_{\theta/a}, G_\theta)$  to see whether the given divergence prefers overdispersion to underdispersion. The average Cramér divergence is improved for all 30 models when initially overdispersed forecasts are made underdispersed, and the average KL divergence is improved for all 30 models when underdispersed forecasts are made overdispersed.

After computing these forecast and target densities, we then performed the following evaluation scheme for each model. At each spatial location, we first shifted the forecast density so that it matches the mean of the target density—this was done to focus on differences in scale. We then estimated the standard deviations of the forecast and target densities, and denote these distributions by  $F_{a\theta}$  and  $G_\theta$ , respectively. Note that if  $a > 1$  then the forecast distribution is overdispersed compared to the target at the given spatial location, and if  $a < 1$  then it is underdispersed. Lastly, subsetting to spatial locations with  $a > 1$ , we computed the average divergence  $d(F_{a\theta}, G_\theta)$ , as well as the average divergence  $d(F_{\theta/a}, G_\theta)$ . The former represents the divergence of the (original) overdispersed forecast, while the latter represents the divergence of the underdispersed counterpart (where the deviation in scale has been inverted). This is displayed on the left panel of Figure 5, where one point represents one model and one divergence—either KL (associated with log loss), or Cramér divergence (associated with CRP loss). The right panel of Figure 5 displays the result of a complementary calculation: subsetting to spatial locations with  $a < 1$ , we compare the average divergence  $d(F_{a\theta}, G_\theta)$  and the average divergence  $d(F_{\theta/a}, G_\theta)$ . We can clearly see that all 30 models from CMIP6 have their overdispersed forecasts improve in Cramér

divergence when deflated and all their underdispersed forecasts improve in KL divergence when inflated.

#### 4.4 Synthetic data

The asymmetric Laplace distribution has density

$$f(x) = \frac{p(1-p)}{\sigma} e^{-\frac{|x-\mu|}{\sigma}(p-\mathbb{I}\{x \leq \mu\})},$$

for  $x \in \mathbb{R}$ , a location parameter  $\mu \in \mathbb{R}$ , a scale parameter  $\sigma > 0$ , and skew parameter  $p \in (0, 1)$  (Koenker and Machado, 1999; Yu and Zhang, 2005). This reduces to the standard Laplace distribution for  $p = 1/2$ , it is skewed to the right for  $p < 1/2$ , and skewed to the left for  $p > 1/2$ . Often used in Bayesian quantile regression (Yu and Moyeed, 2001), it has been more recently employed in probabilistic forecasting, for wind power forecasts (Wang et al., 2022a,b). The purpose of the experiment in this subsection is twofold: it depicts behaviors one would expect given our theoretical results, and also displays interesting phenomena outside of the scope of our theory, pointing towards possible future work.

We computed the CRP, logarithmic, quadratic, spherical, and Dawid–Sebastiani loss between a zero-mean unit-variance target asymmetric Laplace distribution, and forecast distributions in the same family but with varying location and scale. Figure 6 displays the results, with each row showing a different skew parameter, and each column a different loss. The top row corresponds to  $p = 0.2$  (right-skewed), the middle row to  $p = 0.5$  (symmetric), and the bottom row to  $p = 0.8$  (left-skewed). As expected, losses penalize symmetrically on the location  $\mu$  when the scale is correctly specified, except for logarithmic loss—this loss is symmetric in  $\mu$  when the distribution itself is symmetric (middle row), but it prefers upshifted or downshifted forecasts when the distribution is right- or left-skewed (top or bottom rows), respectively.

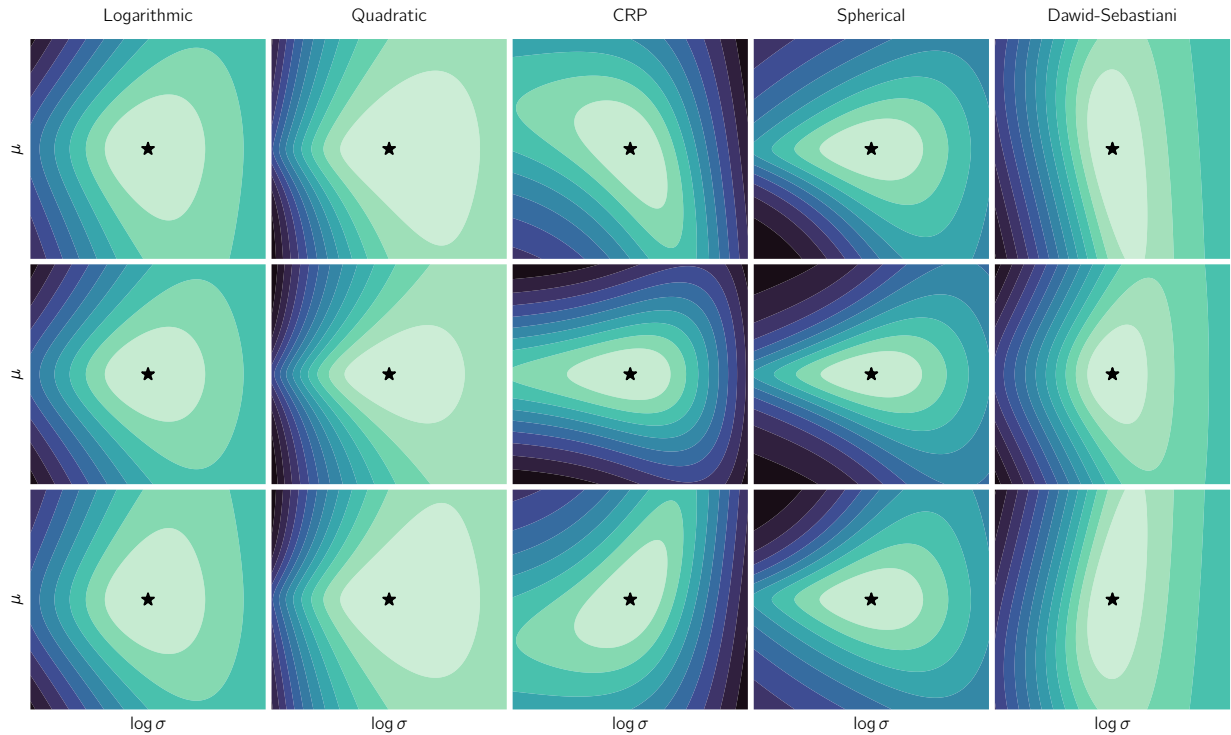


Figure 6: Expected losses for a zero-mean unit-variance asymmetric Laplace target, and forecasts of the same family with varying location  $\mu$  and scale  $\sigma$ . Distributions are right skewed (top panel;  $p = 0.2$ ), symmetric (middle;  $p = 1/2$ ), or left skewed (bottom;  $p = 0.8$ ). A lighter color represents a lower loss, with minimum achieved at the star.

When the location is correctly specified, the penalties on the scale  $\sigma$  all agree with what is suggested by our theory. CRP prefers underdispersed forecasts, log loss prefers underdispersed forecasts in the case without skewness (middle row, in which case we are in an exponential family), quadratic and DS losses prefer overdispersed forecasts, and spherical

loss is symmetric in  $\log \sigma$ . Interestingly, the asymmetric penalty of log loss in the symmetric Laplace case extends to the right- and left-skewed cases (top and bottom rows), despite the fact that the asymmetric Laplace family is not an exponential family. Moreover, considering the behavior of losses in  $\mu, \sigma$  jointly leads to some interesting observations. For example, spherical loss, despite being symmetric on both axes, can become asymmetric in the scale parameter, for misspecified location. As another example, CRP seems particularly affected by skew in the underlying distribution, with its sublevel sets exhibiting a strong tilt in the asymmetric Laplace cases.

## 5 Hedging proper losses under distribution shift

It is commonly held that proper loss functions encourage honest forecasting, in the sense that if a forecaster believes the target distribution is  $G$ , then they can minimize their expected loss by forecasting  $G$ . This statement can be understood in the framework of subjective probability: if  $G$  is the subjective probability of the forecaster, then  $G$  is the conditional distribution of the target given the information available to the forecaster. Propriety guarantees that no other forecast  $F$  will incur lesser (conditional expected) loss,  $\ell(F, G) \geq \ell(G, G)$ . This subjective probability formulation is articulated explicitly in earlier seminal papers (as in [Brier, 1950](#); [Winkler and Murphy, 1968](#)), but not as often in modern ones (as in [Gneiting and Raftery, 2007](#); [Parry et al., 2012](#)). In practice, forecasts are rarely subjective probabilities. This can be attributed to a multitude of issues, such as misspecification of the data generating process. If  $G$  is not the forecaster's subjective probability, then no formal guarantee appears to follow from the definition of propriety that would merit the assertion that the forecaster should forecast their opinion  $G$ .

Consider a forecaster with firm opinion that the target distribution is  $G$ . The forecaster may ask—what if I am wrong? If error is conceivable, the forecaster might then ask—is it better to err in one form over another? If the answer to the latter question is affirmative, the forecaster might be incentivized to deviate from their honest opinion to protect against the possibility of erring in a particularly unfavorable way. Such behavior has been termed *hedging*. A key motivation for using proper losses has historically been the supposition that they provide no opportunity for hedging ([Brier, 1950](#); [Murphy and Epstein, 1967](#); [Winkler and Murphy, 1968](#)).

We are motivated to scrutinize this supposition in situations where forecasting error is possible (or even unavoidable) and losses exhibit asymmetric penalties on forecast errors. In particular, we study hedging in a setting of distribution shift, in which the parameter in a scale or exponential family shifts in testing relative to the training population. In this case, if the shift is log-symmetric around the training parameter value, then the asymmetry in loss penalties can be used to describe the direction toward which the forecaster ought to deviate from their honest opinion.

### 5.1 Problem setting

We suppose that the forecaster has ideal knowledge of the training population, say, by having access to infinitely many independent and identically distributed observations, so they are able to conclude with certainty that the distribution of the target in training is  $G_{\sigma_{\text{train}}}$ . In testing, however, suppose that there is distribution shift in the scale parameter, where the law of target variable  $Y$  in testing is defined as follows: we first draw a random scale parameter  $\sigma_{\text{test}} > 0$ , then draw  $Y \sim G_{\sigma_{\text{test}}}$ . To express our ignorance of the nature of the distribution shift relative to the training population, we assume that  $\sigma_{\text{test}}$  is log-symmetric around  $\sigma_{\text{train}}$ , that is,  $\log \sigma_{\text{test}}$  has a symmetric distribution around  $\log \sigma_{\text{train}}$ .

A forecaster not aware of distribution shift in their data might naively forecast  $G_{\sigma_{\text{train}}}$ . The question then arises whether the forecaster can do better if they suspect distribution shift is present (as would be common in many, if not most, real applications of forecasting). If a loss function  $\ell$  is proper, then the minimum expected loss over all possible realizations of the test scale  $\sigma_{\text{test}}$  is of course obtained by  $\mathbb{E}G_{\sigma_{\text{test}}}$ , the unconditional law of  $Y$ . That is,

$$\mathbb{E}\ell(F, G_{\sigma_{\text{test}}}) \geq \mathbb{E}\ell(\mathbb{E}G_{\sigma_{\text{test}}}, G_{\sigma_{\text{test}}}), \quad \text{for any } F.$$

However, this requires the forecaster to have perfect knowledge of the distribution of  $\sigma_{\text{test}}$ , whereas our setting assumes no such knowledge. The forecaster, equipped only with knowledge of log-symmetry of the test scale distribution, might seek a better forecast than  $G_{\sigma_{\text{train}}}$  within the scale family  $\{G_\sigma : \sigma > 0\}$ , and the question we consider here is whether there is a fixed forecast  $G_{\sigma^*}$  with lesser expected loss. We show that the answer is generally yes.

Before going on to state and prove general results about hedging for the various loss functions, we present an informal discussion that may serve as an intuitive guide relating hedging to asymmetric penalties. The setting of distribution

shift we analyze here differs from the previous setting of asymmetric penalties studied in Section 3, in that the roles of forecast and target distributions are, in a certain sense, reversed. In Section 3, recall, the target  $G = G_1$  was fixed and we considered multiple forecasts  $G_a$  and  $G_{1/a}$  dispersed log-symmetrically around the target. Instead, we now think of a given forecast  $G$  as fixed, and we consider multiple targets dispersed log-symmetrically around the forecast. If  $\sigma_{\text{test}}$  is distributed uniformly on  $\{a, 1/a\}$  with  $a > 1$  (assuming without loss of generality that  $\sigma_{\text{train}} = 1$ ), then

$$2\mathbb{E}d(G, G_{\sigma_{\text{test}}}) = d(G, G_a) + d(G, G_{1/a}).$$

If the divergence is scale invariant, such as the one induced by logarithmic loss, then

$$d(G, G_a) = d(G_{1/a}, G) \quad \text{and} \quad d(G, G_{1/a}) = d(G_a, G).$$

Meaning, penalties are reversed, and based on Theorem 2 the realization  $G_a$  of larger target scale will typically lead to larger divergence. If instead the divergence is symmetric, such as the one induced by CRP or quadratic loss, then

$$d(G, G_a) = d(G_a, G) \quad \text{and} \quad d(G, G_{1/a}) = d(G_{1/a}, G).$$

Lemma 2 tells us that  $G_a$  will lead to larger divergence if  $d$  is rescalable with increasing scale function, as in CRP loss, or will lead to smaller divergence if  $d$  is rescalable with decreasing scale function, as in quadratic loss. In summary, for symmetric divergences the two settings of asymmetric penalties and of distribution shift are interchangeable, whereas for scale invariant divergences they are the reverse of each other.

It may appear at this point that a forecaster would hedge in a direction that draws toward the least favorable realization of the test scale parameter in order to mitigate it, and this is indeed the case for logarithmic, CRP, and quadratic losses in certain cases. However, in general, the precise arguments needed for these (and other) losses are more subtle and we give the details across the next two subsections.

## 5.2 Scale families

The next theorem characterizes the direction of hedging for losses that induce symmetric rescalable divergence, and the direction is shown to depend on the particular scale family. (We make the assumption that the training scale parameter is set to be  $\sigma_{\text{train}} = 1$  here, which we again emphasize comes at no loss of generality.)

**Theorem 4.** *Let  $\{G_\sigma : \sigma > 0\}$  be a scale family,  $\ell$  a loss function, and  $d$  the induced divergence, where  $d$  is symmetric and rescalable with a scaling function  $h$ . Let  $\sigma_{\text{test}} > 0$  be a random variable, which is not almost surely constant, such that  $\sigma_{\text{test}}$  and  $1/\sigma_{\text{test}}$  have the same distribution and  $\mathbb{E}\ell(G_\sigma, G_{\sigma_{\text{test}}})$  is finite for all  $\sigma > 0$ . Fix  $G = G_1$  and define*

$$f(\sigma) = d(G_\sigma, G),$$

*Assume that  $f$  and  $h$  are differentiable and conditions for exchanging differentiation and taking expectation with respect to  $\sigma_{\text{test}}$  apply (e.g., a sufficient condition is that  $\sigma_{\text{test}}$  has compactly supported density and  $f'$  is continuous). Then the following holds.*

1. *If  $(h - 1)/f$  is increasing on  $[1, \infty)$ , then there exists  $\sigma^* < 1$  such that  $\mathbb{E}\ell(G_{\sigma^*}, G_{\sigma_{\text{test}}}) < \mathbb{E}\ell(G, G_{\sigma_{\text{test}}})$ .*
2. *If  $(h - 1)/f$  is decreasing on  $[1, \infty)$ , then there exists  $\sigma^* > 1$  such that  $\mathbb{E}\ell(G_{\sigma^*}, G_{\sigma_{\text{test}}}) < \mathbb{E}\ell(G, G_{\sigma_{\text{test}}})$ .*

*Proof.* Define

$$g_a(\sigma) = d(G_\sigma, G_a) + d(G_\sigma, G_{1/a}).$$

We will first show that  $g'_a(1)$  has the same sign as the derivative of  $(h - 1)/f$  at  $a$ . Indeed, using rescalability (twice), we can rewrite  $g_a(\sigma)$  as

$$g_a(\sigma) = h(a)d(G_{\sigma/a}, G) + \frac{1}{h(a)}d(G_{a\sigma}, G) = h(a)f(\sigma/a) + \frac{1}{h(a)}f(a\sigma).$$

Since  $f$  is differentiable, so is  $g_a$ , and the derivative of  $g_a$  at 1 is

$$g'_a(1) = \frac{h(a)}{a}f'(1/a) + \frac{a}{h(a)}f'(a).$$

Now we relate  $f'(1/a)$  to  $f'(a)$  in order to plug into the equation for  $g'_a(1)$  above. By symmetry and rescalability, note that  $f(\sigma) = h(\sigma)f(1/\sigma)$ , and differentiating this we get

$$f'(\sigma) = h'(\sigma)f(1/\sigma) - \frac{h(\sigma)}{\sigma^2}f'(1/\sigma) = \frac{h'(\sigma)}{h(\sigma)}f(\sigma) - \frac{h(\sigma)}{\sigma^2}f'(1/\sigma).$$

Rearranging to isolate  $f'(1/\sigma)$ , and plugging into the previous equation for  $g'_a(1)$ , we arrive at

$$g'_a(1) = \frac{a}{h(a)}(h'(a)f(a) - (h(a) - 1)f'(a)) = \frac{af(a)^2}{h(a)}\left(\frac{h-1}{f}\right)'(a).$$

The condition that  $(h-1)/f$  is increasing on  $[1, \infty)$  is thus sufficient to ensure a positive derivative  $g'_a(1) > 0$  for all  $a > 1$ . Recalling  $\sigma_{\text{test}}$  is a random variable such that  $\sigma_{\text{test}}$  and  $1/\sigma_{\text{test}}$  have a common distribution, denoted  $H$ , define

$$g(\sigma) = 2\mathbb{E}d(G_\sigma, G_{\sigma_{\text{test}}}) = \mathbb{E}[d(G_\sigma, G_{\sigma_{\text{test}}}) + d(G_\sigma, G_{1/\sigma_{\text{test}}})] = \int g_a(\sigma) dH(a).$$

If differentiation under the integral sign is permitted, then

$$g'(\sigma) = \int g'_a(\sigma) dH(a).$$

The condition that  $(h-1)/f$  is increasing on  $[1, \infty)$  is thus also sufficient to ensure  $g'(1) > 0$ , entailing the existence of  $\sigma^* < 1$  for which

$$\mathbb{E}\ell(G_{\sigma^*}, G_{\sigma_{\text{test}}}) - \mathbb{E}\ell(G, G_{\sigma_{\text{test}}}) = \frac{1}{2}(g(\sigma^*) - g(1)) < 0.$$

The case where  $(h-1)/f$  is decreasing is proven similarly.  $\square$

**Example 1** (Exponential distribution). When  $G_\sigma$  is the exponential distribution with scale  $\sigma$  (see Section 3.3), we can infer the following using Theorem 4. Under CRP loss, hedging is carried out by inflating the scale, making it flatter and less informative, while under quadratic loss it is carried out by deflating the scale, making it sharper and overconfident. To see this, we note a simple calculation yields for CRP loss that

$$d(G_\sigma, G) = (1 + \sigma)/2 - 2\sigma/(1 + \sigma).$$

Recalling  $h(\sigma) = \sigma$ , it may be shown that  $d(G_\sigma, G)/(h(\sigma) - 1)$  is increasing. Hence by Theorem 4, there is a forecast  $G_{\sigma^*}$  flatter than  $G$  (i.e.,  $\sigma^* > 1$ ) which attains lower expected CRP loss. For quadratic loss, a simple calculation yields

$$d(G_\sigma, G) = (\sigma - 1)^2/(2\sigma(\sigma + 1)).$$

Recalling  $h(\sigma) = 1/\sigma$ , it may be shown that  $(h(\sigma) - 1)/d(G_\sigma, G)$  is increasing. Thus by Theorem 4, there is a forecast  $G_{\sigma^*}$  sharper than  $G$  (i.e.,  $\sigma^* < 1$ ) which attains lower expected quadratic loss.

### 5.3 Exponential families

For logarithmic loss, the divergence it induces is not symmetric, but we can characterize the direction of hedging with a specialized argument for exponential families.

**Theorem 5.** *Let  $\{p_\eta : \eta > 0\}$  be a minimal exponential family of densities, where  $p_\eta(x) = h(x)e^{\eta T(x) - A(\eta)}$ . Denote by  $\ell$  the logarithmic loss, and let  $\eta_{\text{test}} > 0$  be a random variable where we assume  $\mathbb{E}T(Y)$  exists and is finite, where  $Y$  is a random variable whose conditional distribution given  $\eta_{\text{test}}$  is  $p_{\eta_{\text{test}}}$ . Then  $\eta^* = (A')^{-1}(\mathbb{E}A'(\eta_{\text{test}}))$  is well-defined and minimizes then the expected loss  $\mathbb{E}\ell(p_\eta, p_{\eta_{\text{test}}})$  over all  $\eta > 0$ .*

*Proof.* We first show that  $\eta^*$  is well-defined. Recall, for a minimal exponential family, the log-partition function  $A$  is continuously differentiable and strictly convex (Wainwright and Jordan, 2008), and  $A'$  acts as a bijection between its domain and image (Rockafellar, 1970), which must then be an open interval. Furthermore, by a standard identity for exponential families,

$$\mathbb{E}T(Y) = \mathbb{E}[\mathbb{E}T(Y)|\eta_{\text{test}}] = \mathbb{E}A'(\eta_{\text{test}}).$$

By assumption, this value is finite, and thus the expectation  $\mathbb{E}A'(\eta_{\text{test}})$  must lie within the image of  $A'$ , which implies the existence and uniqueness of  $\eta^*$  for which  $A'(\eta^*) = \mathbb{E}A'(\eta_{\text{test}})$ . It remains to show that  $\eta^*$  minimizes the expected logarithmic loss by completing the Bregman divergence. We can compute the expected loss for any  $\eta > 0$  by

$$\mathbb{E}\ell(p_\eta, p_{\eta_{\text{test}}}) = -\mathbb{E}[\mathbb{E} \log p_\eta(Y) | \eta_{\text{test}}] = A(\eta) - \eta \mathbb{E}T(Y) + c = A(\eta) - \eta A'(\eta^*) + c,$$

where  $c$  is constant. The difference in expected loss between  $\eta$  and  $\eta^*$  is therefore

$$\mathbb{E}\ell(p_\eta, p_{\eta_{\text{test}}}) - \mathbb{E}\ell(p_{\eta^*}, p_{\eta_{\text{test}}}) = A(\eta) - A(\eta^*) - (\eta - \eta^*)A'(\eta^*).$$

This is the Bregman divergence of the strictly convex function  $A$ , tangent to  $A$  at  $\eta^*$ , which is nonnegative and vanishes if and only if  $\eta = \eta^*$ .  $\square$

No assumption was required so far on the relation between  $\eta_{\text{train}}$  and  $\eta_{\text{test}}$ , the natural parameters in training and testing. If we assume  $\eta_{\text{test}}$  is logarithmically symmetric around  $\eta_{\text{train}}$ , then

$$\eta_{\text{train}} = e^{\mathbb{E} \log(\eta_{\text{test}})}.$$

Compare this with the optimal forecast from the theorem:

$$\eta^* = (A')^{-1}(\mathbb{E}A'(\eta_{\text{test}})).$$

We see that whether  $\eta^* < \eta_{\text{train}}$  or  $\eta^* > \eta_{\text{train}}$  holds will depend on the log-partition function  $A$ . We conclude this subsection with an example where this occurs.

**Example 2** (Generalized gamma scale family). When  $p_\eta$  is the generalized gamma density (see Section 3.3), with scale  $\sigma$  inversely proportional to  $\eta$ , we can infer the following from Theorem 5. Under logarithmic loss, hedging is carried out by inflating the scale relative to the training population. To see this, recall that for the generalized gamma family  $\eta = 1/\sigma^\gamma$  with  $\gamma > 0$ , and the log-partition function has derivative  $A'(\eta) = -(k/\gamma)/\eta$ . The natural parameter  $\eta^*$  for which the forecast  $p_{\eta^*}$  attains global minimum expected logarithmic loss is

$$\frac{1}{\eta^*} = \mathbb{E} \left[ \frac{1}{\eta_{\text{test}}} \right].$$

Now compare the optimal scale  $\sigma^* = (\eta^*)^{-1/\gamma}$  with the training scale  $\sigma_{\text{train}} = (\eta_{\text{train}})^{-1/\gamma}$ : using Jensen's inequality,

$$(\sigma^*)^{-\gamma} = \eta^* = (\mathbb{E}\eta_{\text{test}}^{-1})^{-1} < e^{\mathbb{E} \log(\eta_{\text{test}})} = \eta_{\text{train}} = \sigma_{\text{train}}^{-\gamma},$$

which shows that  $\sigma^* > \sigma_{\text{train}}$ . From special cases of the generalized gamma scale family, we may derive results for the exponential, Laplace, normal, gamma, and Weibull scale families.

## 6 Discussion

In this work, we studied asymmetries in the penalization of a broad set of proper loss functions, including logarithmic, continuous ranked probability, threshold-weighted CRP, quadratic, spherical, energy, and Dawid–Sebastiani losses. To recap some highlights, by establishing general results in exponential families for logarithmic loss, we showed this loss typically penalizes overestimating scale parameters less severely than underestimating them by the same amount on a logarithmic scale. Moreover, by introducing the notion of symmetric rescalable divergences, we showed that in scale families CRP loss favors sharp forecasts (underestimating the scale), whereas quadratic loss favors flat forecasts (overestimating the scale). These results are clearly visible in practice: through experiments, we confirmed the effects anticipated by the theory on data from Covid-19 mortality, temperature, and retail forecasts. Finally, under a setting with distribution shift, we showed that hedging of certain proper loss functions is possible, which can be understood as an implication of their inherent asymmetry.

We close with some additional related comments and discussion.

## 6.1 Confounding effects of aggregation across different scales

In practice, a loss is often averaged over non-identically distributed target observations, for example, to evaluate average performance of a forecaster across different dates, geographic locations, or generally over different tasks. The problem of confounding effects stemming from the differences between the tasks is well-recognized, with skill losses a popular yet imperfect remedy (Gneiting and Raftery, 2007). Here we note that the confounding effects of scale can depend on the loss function being used, and the asymmetries therein.

We demonstrate via two examples that losses which induce symmetric rescalable divergences with increasing scaling functions (e.g., CRP and energy) place more weight on observations with large scale versus those with small scale, and losses with decreasing scaling function (e.g., quadratic) behave in the opposite way. On the other hand, losses with constant scaling function (e.g., logarithmic and DS) are indifferent to the scale of the target.

**Example 3** (Different specializations). Consider two tasks with different scale, and two forecasters, Glenn and Bob. Glenn is relatively good in forecasting one task, and Bob equally better in the other. We show that which forecaster is awarded least expected loss depends on the loss function being used. Concretely, in one task with the target distribution being  $G$ , suppose that Glenn forecasts  $F$  and Bob  $H$ , and Glenn achieves lower expected loss,

$$\ell(F, G) < \ell(H, G).$$

However, in another task with target distribution  $G_\sigma$ , suppose that in a reversal Bob now forecasts  $F_\sigma$  and Glenn  $H_\sigma$ . Here, the distributions  $F_\sigma, G_\sigma, H_\sigma$  should be read as members of respective scale families, where we assume  $\sigma > 1$  to signify increased scale. If the divergence induced by  $\ell$  is symmetric and rescalable with constant scaling function (e.g., logarithmic and DS), it is indifferent to the scale of the second task and assigns equal expected loss to Glenn and Bob in total over both tasks,

$$\ell(F, G) + \ell(H_\sigma, G_\sigma) = \ell(H, G) + \ell(F_\sigma, G_\sigma).$$

However, when the divergence has increasing scaling function (e.g., CRP and energy), more emphasis is placed on the second upscaled task, and consequently Bob wins:

$$\ell(F, G) + \ell(H_\sigma, G_\sigma) > \ell(H, G) + \ell(F_\sigma, G_\sigma).$$

Lastly, if the divergence has decreasing scaling function (e.g., quadratic, and also spherical when  $F, G, H$  belong to the same scale family), lesser weight is put on the second task due to its increased scale, and Glenn wins:

$$\ell(F, G) + \ell(H_\sigma, G_\sigma) < \ell(H, G) + \ell(F_\sigma, G_\sigma).$$

We have reached three different conclusions by using different loss functions, with all else being equal.

**Example 4** (Missing forecasts). In this example, Glenn and Bob make the same forecasts, but Bob is missing forecasts for some target observations. (Missingness is common in some domains, e.g., in epidemiological forecasting; Cramer et al. (2022b) report that only 28 out of 71 forecasters of Covid-19 mortality submitted full forecasts for at least 60% of participating weeks in their analysis.) Concretely, in the first task, suppose that both Glenn and Bob forecast  $F$ , when the target distribution is  $G$ . In the second task, suppose Glenn forecasts  $F_\sigma$ , and the target distribution is  $G_\sigma$  with  $\sigma > 1$ , however, Bob makes no forecast. Which forecaster is awarded the least expected loss—now averaged over the observed forecasts—depends on the loss function being used. If the divergence induced by  $\ell$  is symmetric and rescalable with constant scaling function (e.g., logarithmic and DS), then expected loss at the second task equals that at the first task,

$$\frac{\ell(F, G) + \ell(F_\sigma, G_\sigma)}{2} = \ell(F, G),$$

and neither Glenn nor Bob wins. If, however, the divergence has increasing scaling function (e.g., CRP and energy), then the loss at the second task is greater, leading to Bob winning:

$$\frac{\ell(F, G) + \ell(F_\sigma, G_\sigma)}{2} > \ell(F, G).$$

Conversely, if the divergence has decreasing scaling function (e.g., quadratic, and also spherical when  $F, G$  belong to the same scale family), then the loss at the second task is lesser, leading to Glenn winning:

$$\frac{\ell(F, G) + \ell(F_\sigma, G_\sigma)}{2} < \ell(F, G).$$

Once again, we see that three different conclusions have been reached by using different loss functions.

## 6.2 A closer look at logarithmic loss in exponential families

In Section 3.3, we considered densities  $p_\eta(x) = h(x)e^{\eta T(x) - A(\eta)}$  in the exponential family  $\{p_\eta : \eta > 0\}$  and proved, for  $\theta > 1$  and  $\ell$  being the logarithmic loss, that  $\ell(p_{\theta\eta}, p_\eta) - \ell(p_{\eta/\theta}, p_\eta)$  is positive, negative, or zero when  $\eta^3 A''(\eta)$  is respectively increasing, decreasing, or constant. Instead of setting a parametrization a priori (i.e., comparing  $\theta\eta$  to  $\eta/\theta$ ), one may instead ask about the sign of  $\ell(p_{\eta_1}, p_\eta) - \ell(p_{\eta_2}, p_\eta)$  for varying  $\eta_1$ , with  $\eta_2, \eta$  fixed. Figure 7 visualizes this quantity for the normal scale family, and Theorem 6 provides a precise characterization for a wide class of distributions, which includes the normal scale family, log-normal log-scale family, exponential family, Weibull scale family, Laplace scale family, gamma scale family, and others.

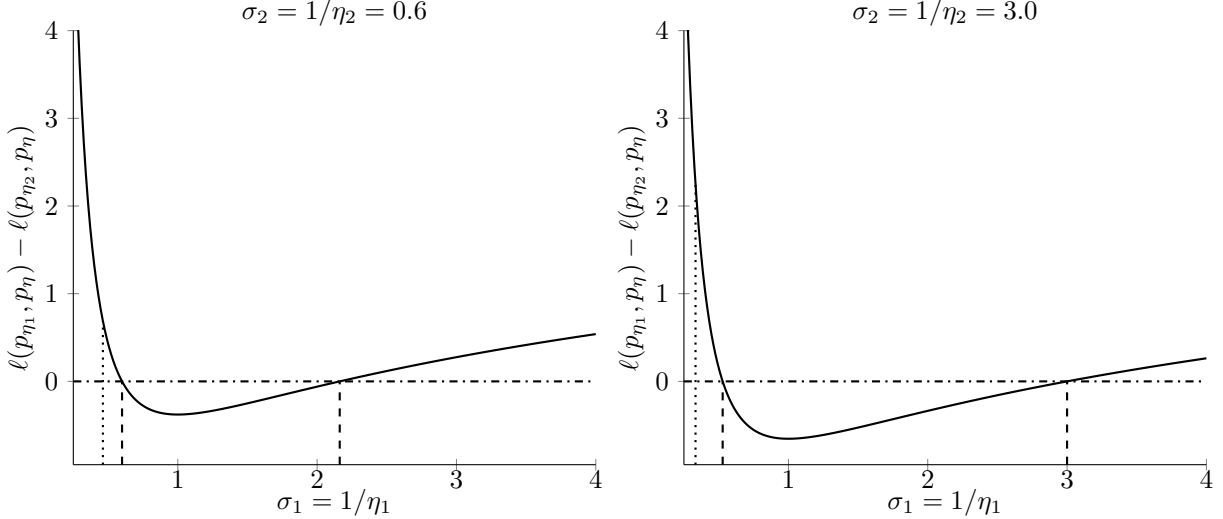


Figure 7: The function  $\ell(p_{\eta_1}, p_\eta) - \ell(p_{\eta_2}, p_\eta)$  for normal densities with distinct fixed values of  $\sigma_2$  (solid), the roots given by Theorem 6 in terms of the Lambert function (dashed) and the multiplicative inverse of the largest of the two roots (dotted).

**Theorem 6.** *For an exponential family  $\{p_\eta : \eta > 0\}$  with log-partition function of the form  $A(\eta) = c_1 \log \eta + c_2$ , for constants  $c_1, c_2 \in \mathbb{R}$ , the roots of  $\ell(p_{\eta_1}, p_\eta) - \ell(p_{\eta_2}, p_\eta)$  occur at*

$$-\eta W\left(-\frac{\eta_2}{\eta} \exp\left(-\frac{\eta_2}{\eta}\right)\right),$$

where  $W : [-\frac{1}{e}, \infty) \rightarrow \mathbb{R}^2$  is the Lambert function, which satisfies the implicit equation  $x = W(x) \exp(W(x))$ .

*Proof.* Representing the difference of logarithmic losses by the equivalent difference of KL divergences yields

$$\ell(p_{\eta_1}, p_\eta) - \ell(p_{\eta_2}, p_\eta) = d(p_{\eta_1}, p) - d(p_{\eta_2}, p_\eta) = \mathbb{E} \log \frac{p_{\eta_2}(Y)}{p_{\eta_1}(Y)} = A(\eta_1) - A(\eta_2) - (\eta_1 - \eta_2) \mathbb{E} T(Y),$$

where  $Y$  is a random variable with density  $p_\eta$ . From the exponential family identity  $\mathbb{E}_\eta T(Y) = A'(\eta)$ , we have

$$\ell(p_{\eta_1}, p_\eta) - \ell(p_{\eta_2}, p_\eta) = A(\eta_1) - A(\eta_2) - (\eta_1 - \eta_2) A'(\eta) = c_1 \log \eta_1 - c_1 \log \eta_2 - \frac{c_1}{\eta} (\eta_1 - \eta_2).$$

Setting the above display to zero gives  $\log \frac{\eta_1}{\eta_2} = \frac{\eta_1 - \eta_2}{\eta}$ . After rearranging and taking exponents, we have

$$\exp(\eta_1) \exp(-\eta \log \eta_1) = \exp(\eta_2) \exp(-\eta \log \eta_2).$$

Exponentiating by  $-\frac{1}{\eta}$  and then multiplying by  $-\frac{1}{\eta}$ , gives

$$-\frac{\eta_1}{\eta} \exp\left(-\frac{\eta_1}{\eta}\right) = -\frac{\eta_2}{\eta} \exp\left(-\frac{\eta_2}{\eta}\right),$$

from which the Lambert function is immediately recognized, yielding

$$-\frac{\eta_1}{\eta} = W\left(-\frac{\eta_2}{\eta} \exp\left(-\frac{\eta_2}{\eta}\right)\right).$$

The result follows by multiplying both sides by  $-\eta$ .  $\square$

### 6.3 Threshold-weighted continuous ranked probability loss

In the introduction and throughout the paper, we alluded to results available for threshold-weighted CRP loss. Here we present the details, for weights of the form  $w(y) = y^\alpha$  with  $\alpha \in \mathbb{R}$ , subject to  $w$  remaining nonnegative (power-weighted CRP loss). This loss has asymmetries in location and scale families governed by the exponent  $\alpha$ . Indeed, as a direct consequence of Lemma 1, for  $\{G_\sigma : \sigma > 0\}$  a scale family,  $\sigma > 0$ , and  $\ell$  a power-weighted CRP loss, we have:

- $\ell(G_\sigma, G) = \ell(G_{1/\sigma}, G)$  if  $\alpha = -1$ ;
- $\ell(G_\sigma, G) > \ell(G_{1/\sigma}, G)$  if  $\alpha > -1$ ;
- $\ell(G_\sigma, G) < \ell(G_{1/\sigma}, G)$  if  $\alpha < -1$ .

Moreover, for  $\{G_\mu : \mu \in \mathbb{R}\}$  a location family, by a similar argument, we have:

- $\ell(G_\mu, G) = \ell(G_{-\mu}, G)$  if  $\alpha = 0$  or  $\mu = 0$ ;
- $\ell(G_\mu, G) > \ell(G_{-\mu}, G)$  if  $\text{sign}(\alpha) = \text{sign}(\mu) \neq 0$ ;
- $\ell(G_\mu, G) < \ell(G_{-\mu}, G)$  otherwise.

We conclude that power-weighted CRP loss has an inherent trade-off: it can penalize symmetrically in location families at the expense of asymmetry in scale families ( $\alpha = 0$ ), or it can penalize symmetrically in scale families at the expense of asymmetry in location families ( $\alpha = -1$ ). There is no power weight function that guarantees symmetric penalties in both families simultaneously. A natural question is now whether there exists a weight function, not necessarily a power function, that wholly symmetrizes CRP loss in this context. Our next results answers this in the negative, apart from the trivial zero function.

**Proposition 1.** *Let  $\{G_\sigma : \sigma > 0\}$  and  $\{G_\mu : \mu \in \mathbb{R}\}$  be scale and location families, respectively. For the threshold-weighted CRP loss  $\ell$ ,*

$$\ell(G_\sigma, G_1) = \ell(G_{1/\sigma}, G_1) \text{ and } \ell(G_\mu, G_0) = \ell(G_{-\mu}, G_0), \text{ for all } \sigma > 0, \mu \in \mathbb{R} \iff w(y) = 0, \text{ for all } y \in \mathcal{Y}.$$

*In other words, there does not exist a nonzero weight function such that symmetry is achieved for a location and scale family simultaneously.*

*Proof.* The “if” direction is obvious. For the “only if” direction, observe that  $\ell(G_\sigma, G) = \ell(G_{1/\sigma}, G)$  implies

$$\int_{\mathcal{Y}} \sigma w(y\sigma)(G(y) - G(y\sigma))^2 dy = \int_{\mathcal{Y}} w(y)(G(y) - G(y\sigma))^2 dy \implies \sigma w(y\sigma) = w(y),$$

whereas  $\ell(G_\mu, G) = \ell(G_{-\mu}, G)$  implies

$$\int_{\mathcal{Y}} w(y + \mu)(G(y) - G(y + \mu))^2 dy = \int_{\mathcal{Y}} w(y)(G(y) - G(y + \mu))^2 dy \implies w(y + \mu) = w(y).$$

The only weight function that satisfies both conditions for all  $\sigma > 0$  and  $\mu \in \mathbb{R}$  is the zero function:  $w(y) = 0$  for all  $y \in \mathcal{Y}$ .  $\square$

Therefore, the trade-off between ensuring symmetric penalties either in location or in scale families is not a peculiarity of power-weighted CRP loss, but extends to the more general threshold-weighted version. In this particular sense, CRP loss is unsymmetrizable. Exploring whether quantile-weighted CRP loss behaves similarly remains an avenue for future work.

## Acknowledgements

We thank members of the Delphi research group, as well as Tilmann Gneiting, Evan Ray, and Nicholas Reich for useful discussions. We also thank the participants of the Berkeley Statistics probabilistic forecasting reading group. This work was supported by Centers for Disease Control and Prevention (CDC) grant number 75D30123C15907.

## References

Sam Allen, Jonas Bhend, Olivia Martius, and Johanna Ziegel. Weighted verification tools to evaluate univariate and multivariate probabilistic forecasts for high-impact weather events. *Weather and Forecasting*, 38(3):499–516, 2023a.

Sam Allen, David Ginsbourger, and Johanna Ziegel. Evaluating forecasts for high-impact events using transformed kernel scores. *SIAM/ASA Journal on Uncertainty Quantification*, 11(3):906–940, 2023b.

Gianni Amisano and Raffaella Giacomini. Comparing density forecasts via weighted likelihood ratio tests. *Journal of Business & Economic Statistics*, 25(2):177–190, 2007.

George B. Arfken, Hans J. Weber, and Frank E. Harris. *Mathematical Methods for Physicists: A Comprehensive Guide*. Academic Press, 2011.

Ludwig Baringhaus and Carsten Franz. On a new multivariate two-sample test. *Journal of Multivariate Analysis*, 88(1):190–206, 2004.

Riccardo Benedetti. Scoring rules for forecast verification. *Monthly Weather Review*, 138(1):203–211, 2010.

José M. Bernardo. Expected information as expected utility. *Annals of Statistics*, 7(3):686–690, 1979.

J. Eric Bickel. Some comparisons among quadratic, spherical, and logarithmic scoring rules. *Decision Analysis*, 4(2):49–65, 2007.

Johannes Bracher, Evan L. Ray, Tilmann Gneiting, and Nicholas G. Reich. Evaluating epidemic forecasts in an interval format. *PLOS Computational Biology*, 17(2):1–15, 2021.

Glenn W. Brier. Verification of forecasts expressed in terms of probability. *Monthly Weather Review*, 78(1):1–3, 1950.

Andreas Buja, Werner Stuetzle, and Yi Shen. Loss functions for binary class probability estimation and classification: Structure and applications. Technical Report, The Wharton School, University of Pennsylvania, 2005.

Arthur Carvalho. An overview of applications of proper scoring rules. *Decision Analysis*, 13(4):223–242, 2016.

Dombry Clement and Ahmed Zaoui. Distributional regression: CRPS-error bounds for model fitting, model selection and convex aggregation. In *Advances in Neural Information Processing Systems*, 2024.

Estee Y. Cramer, Yuxin Huang, Yijin Wang, Evan L. Ray, Matthew Cornell, Johannes Bracher, Andrea Brennen, Alvaro J. Castro Rivadeneira, Aaron Gerdling, Katie H. House, et al. The United States COVID-19 Forecast Hub dataset. *Scientific Data*, 9, 2022a.

Estee Y. Cramer, Evan L. Ray, Velma K. Lopez, Johannes Bracher, Andrea Brennen, Alvaro J. Castro Rivadeneira, Aaron Gerdling, Tilmann Gneiting, Katie H. House, Yuxin Huang, et al. Evaluation of individual and ensemble probabilistic forecasts of COVID-19 mortality in the United States. *Proceedings of the National Academy of Sciences*, 119(15):e2113561119, 2022b.

Harald Cramér. On the composition of elementary errors. *Scandinavian Actuarial Journal*, 1928(1):141–180, 1928.

A. Philip Dawid. Present position and potential developments: Some personal views statistical theory the prequential approach. *Journal of the Royal Statistical Society: Series A*, 147(2):278–290, 1984.

A. Philip Dawid. The geometry of proper scoring rules. *Annals of the Institute of Statistical Mathematics*, 59:77–93, 2007.

A. Philip Dawid and Paola Sebastiani. Coherent dispersion criteria for optimal experimental design. *Annals of Statistics*, pages 65–81, 1999.

Bruno de Finetti. *Theory of Probability*. John Wiley & Sons, 1975.

Alexander Dietmüller, Albert Gran Alcoz, and Laurent Vanbever. FitNets: An adaptive framework to learn accurate traffic distributions. arXiv: 2405.10931, 2024.

Robert J. H. Dunn, Lisa V. Alexander, Markus G. Donat, Xuebin Zhang, Margot Bador, Nicholas Herold, et al. Development of an updated global land in situ-based data set of temperature and precipitation extremes: HadEX3. *Journal of Geophysical Research: Atmospheres*, 125(16):e2019JD032263, 2020.

Werner Ehm, Tilmann Gneiting, Alexander Jordan, and Fabian Krüger. Of quantiles and expectiles: Consistent scoring functions, Choquet representations and forecast rankings. *Journal of the Royal Statistical Society: Series B*, 78(3): 505–562, 2016.

Veronika Eyring, Sandrine Bony, Gerald A. Meehl, Catherine A. Senior, Bjorn Stevens, Ronald J. Stouffer, and Karl E. Taylor. Overview of the Coupled Model Intercomparison Project Phase 6 (CMIP6) experimental design and organization. *Geoscientific Model Development*, 9(5):1937–1958, 2016.

Kira Feldmann, Michael Scheuerer, and Thordis L. Thorarinsdottir. Spatial postprocessing of ensemble forecasts for temperature using nonhomogeneous gaussian regression. *Monthly Weather Review*, 143(3):955–971, 2015.

Jerome Friedman. Greedy function approximation: A gradient boosting machine. *Annals of Statistics*, 29(5):1190–1232, 2001.

John W. Galbraith and Simon van Norden. Assessing gross domestic product and inflation probability forecasts derived from bank of england fan charts. *Journal of the Royal Statistical Society: Series A*, 175(3):713–727, 2012.

Tilmann Gneiting and Matthias Katzfuss. Probabilistic forecasting. *Annual Review of Statistics and Its Application*, 1: 125–151, 2014.

Tilmann Gneiting and Adrian E. Raftery. Strictly proper scoring rules, prediction, and estimation. *Journal of the American Statistical Association*, 102(477):359–378, 2007.

Tilmann Gneiting and Roopesh Ranjan. Comparing density forecasts using threshold- and quantile-weighted scoring rules. *Journal of Business & Economic Statistics*, 29(3):411–422, 2011.

Tilmann Gneiting, Adrian E. Raftery, Anton H. Westveld, and Tom Goldman. Calibrated probabilistic forecasting using ensemble model output statistics and minimum CRPS estimation. *Monthly Weather Review*, 133(5):1098–1118, 2005.

Tilmann Gneiting, Fadoua Balabdaoui, and Adrian E. Raftery. Probabilistic forecasts, calibration and sharpness. *Journal of the Royal Statistical Society: Series B*, 69(2):243–268, 2007.

I. J. Good. Rational decisions. *Journal of the Royal Statistical Society: Series B*, 14(1):107–114, 1952.

I. J. Good. Comment on “Measuring information and uncertainty,” by R. J. Buehler. In *Foundations of Statistical Inference*, pages 337–339. Holt, Rinehart and Winston of Canada, 1971.

Alexander Henzi, Johanna F. Ziegel, and Tilmann Gneiting. Isotonic distributional regression. *Journal of the Royal Statistical Society Series B: Statistical Methodology*, 83(5):963–993, 2021.

Tao Hong, Pierre Pinson, Shu Fan, Hamidreza Zareipour, Alberto Troccoli, and Rob J. Hyndman. Probabilistic energy forecasting: Global energy forecasting competition 2014 and beyond. *International Journal of forecasting*, 32(3): 896–913, 2016.

Stephen C. Hora and Erim Kardeş. Calibration, sharpness and the weighting of experts in a linear opinion pool. *Annals of Operations Research*, 229(1):429–450, 2015.

Ian T. Jolliffe and David B. Stephenson. *Forecast Verification: A Practitioner's Guide in Atmospheric Science*. John Wiley & Sons, 2012.

Thomas H. Jordan, Yun-Tai Chen, Paolo Gasparini, Raul Madariaga, Ian Main, Warner Marzocchi, Gerassimos Papadopoulos, Gennady Sobolev, Koshun Yamaoka, and Jochen Zschau. Operational earthquake forecasting: State of knowledge and guidelines for utilization. *Annals of Geophysics*, 54(4):315–391, 2011.

Robert W. Keener. *Theoretical Statistics: Topics for a Core Course*. Springer, 2010.

Seung-Jean Kim, Kwangmoo Koh, Stephen Boyd, and Dimitry Gorinevsky.  $\ell_1$  trend filtering. *SIAM Review*, 51(2):339–360, 2009.

Dmitrii Kochkov, Janni Yuval, Ian Langmore, Peter Norgaard, Jamie Smith, Griffin Mooers, Milan Klöwer, James Lottes, Stephan Rasp, Peter Düben, et al. Neural general circulation models for weather and climate. *Nature*, 632(8027):1060–1066, 2024.

Roger Koenker and José A. F. Machado. Goodness of fit and related inference processes for quantile regression. *Journal of the American Statistical Association*, 94(448):1296–1310, 1999.

Solomon Kullback and Richard A. Leibler. On information and sufficiency. *Annals of Mathematical Statistics*, 22(1):79–86, 1951.

Francesco Laio and Stefania Tamea. Verification tools for probabilistic forecasts of continuous hydrological variables. *Hydrology and Earth System Sciences*, 11:1267–1277, 2007.

Kyungmin Lee and Hyeongkeun Lee. Pseudo-spherical knowledge distillation. In *Proceedings of the International Joint Conference on Artificial Intelligence*, 2022.

Sebastian Lerch, Thordis L. Thorarinsdottir, Francesco Ravazzolo, and Tilmann Gneiting. Forecaster's dilemma: Extreme events and forecast evaluation. *Statistical Science*, 32(1):106–127, 2017.

Martin Leutbecher and Tim N. Palmer. Ensemble forecasting. *Journal of Computational Physics*, 227(7):3515–3539, 2008.

Reason L. Machete. Contrasting probabilistic scoring rules. *Journal of Statistical Planning and Inference*, 143(10):1781–1790, 2013.

Spyros Makridakis, Allan Andersen, Robert Carbone, Robert Fildes, Michèle Hibon, Rudolf Lewandowski, Joseph Newton, Emanuel Parzen, and Robert L. Winkler. The accuracy of extrapolation (time series) methods: Results of a forecasting competition. *Journal of Forecasting*, 1(2):111–153, 1982.

Spyros Makridakis, Evangelos Spiliotis, Vassilios Assimakopoulos, Zhi Chen, Anil Gaba, Ilia Tsetlin, and Robert L. Winkler. The M5 uncertainty competition: Results, findings and conclusions. *International Journal of Forecasting*, 38(4):1365–1385, 2022.

James E. Matheson and Robert L. Winkler. Scoring rules for continuous probability distributions. *Management Science*, 22(10):1087–1096, 1976.

Gerald A. Meehl, George J. Boer, Curt Covey, Mojib Latif, and Ronald J. Stouffer. Intercomparison makes for a better climate model. *Eos, Transactions American Geophysical Union*, 78(41):445–451, 1997.

Edgar C. Merkle and Mark Steyvers. Choosing a strictly proper scoring rule. *Decision Analysis*, 10(4):292–304, 2013.

Sebastian Meyer and Leonhard Held. Power-law models for infectious disease spread. *Annals of Applied Statistics*, 3(8):1612–1639, 2014.

Allan H. Murphy and Edward S. Epstein. A note on probability forecasts and “hedging”. *Journal of Applied Meteorology*, 6(6):1002–1004, 1967.

Frank Nielsen. On the Kullback-Leibler divergence between location-scale densities. arXiv: 1904.10428, 2019.

Florian Pappenberger, Jutta Thielen, and Mauro Del Medico. The impact of weather forecast improvements on large scale hydrology: Analysing a decade of forecasts of the European Flood Alert System. *Hydrological Processes*, 25(7):1091–1113, 2011.

Matthew Parry, A. Philip Dawid, and Steffen Lauritzen. Proper local scoring rules. *Annals of Statistics*, 40(1):561–592, 2012.

Andrew J. Patton. Comparing possibly misspecified forecasts. *Journal of Business & Economic Statistics*, 38(4):796–809, 2020.

Adrian E. Raftery and Hana Ševčíková. Probabilistic population forecasting: Short to very long-term. *International Journal of Forecasting*, 39(1):73–97, 2023.

Stephan Rasp and Sebastian Lerch. Neural networks for postprocessing ensemble weather forecasts. *Monthly Weather Review*, 146(11):3885–3900, 2018.

Nicholas G. Reich, Logan C. Brooks, Spencer J. Fox, Sasikiran Kandula, Craig J. McGowan, Evan Moore, Dave Osthus, Evan L. Ray, Abhinav Tushar, Teresa K. Yamana, et al. A collaborative multiyear, multimodel assessment of seasonal influenza forecasting in the united states. *Proceedings of the National Academy of Sciences*, 116(8):3146–3154, 2019.

Johannes Resin, Daniel Wolffram, Johannes Bracher, and Timo Dimitriadis. Shift-dispersion decompositions of Wasserstein and Cramér distances. arXiv: 2408.09770, 2024.

Thornton B. Roby. Belief states and the uses of evidence. *Behavioral Science*, 10(3):255–270, 1965.

R. Tyrrell Rockafellar. *Convex Analysis*. Princeton University Press, 1970.

Leonard J. Savage. Elicitation of personal probabilities and expectations. *Journal of the American Statistical Association*, 66(336):783–801, 1971.

Michael Scheuerer and Thomas M. Hamill. Variogram-based proper scoring rules for probabilistic forecasts of multivariate quantities. *Monthly Weather Review*, 143(4):1321–1334, 2015.

Michael Scheuerer and David Möller. Probabilistic wind speed forecasting on a grid based on ensemble model output statistics. *Annals of Applied Statistics*, 9(3):1328–1349, 2015.

Danijel Schorlemmer, Maximilian J. Werner, Warner Marzocchi, Thomas H. Jordan, Yoshihiko Ogata, David D. Jackson, Sum Mak, David A. Rhoades, Matthew C. Gerstenberger, Naoshi Hirata, et al. The collaboratory for the study of earthquake predictability: Achievements and priorities. *Seismological Research Letters*, 89(4):1305–1313, 2018.

Uwe Schulzweida. CDO user guide, October 2023. URL <https://doi.org/10.5281/zenodo.10020800>.

David W. Scott. *Multivariate Density Estimation: Theory, Practice, and Visualization*. Wiley, 1992.

Reinhard Selten. Axiomatic characterization of the quadratic scoring rule. *Experimental Economics*, 1:43–61, 1998.

Chenze Shao, Fandong Meng, Yijin Liu, and Jie Zhou. Language generation with strictly proper scoring rules. In *Proceedings of the International Conference on Machine Learning*, 2024.

Christopher G. Small. *Functional Equations and How to Solve Them*. Springer, 2007.

Gábor J. Székely and Maria L. Rizzo. A new test for multivariate normality. *Journal of Multivariate Analysis*, 93(1):58–80, 2005.

Gábor J. Székely and Maria L. Rizzo. Energy statistics: A class of statistics based on distances. *Journal of statistical planning and inference*, 143(8):1249–1272, 2013.

Maxime Taillardat, Anne-Laure Fougères, Philippe Naveau, and Raphaël de Fondeville. Evaluating probabilistic forecasts of extremes using continuous ranked probability score distributions. *International Journal of Forecasting*, 39(3):1448–1459, 2023.

Thordis L. Thorarinsdottir, Jana Sillmann, Marion Haugen, Nadine Gissibl, and Marit Sandstad. Evaluation of CMIP5 and CMIP6 simulations of historical surface air temperature extremes using proper evaluation methods. *Environmental Research Letters*, 15(12):124041, December 2020.

Ryan J. Tibshirani. Adaptive piecewise polynomial estimation via trend filtering. *Annals of Statistics*, 42(1):285–323, 2014.

Martin J. Wainwright and Michael I. Jordan. Graphical models, exponential families, and variational inference. *Foundations and Trends in Machine Learning*, 1(1–2):1–305, 2008.

Yun Wang, Tuo Chen, Runmin Zou, Dongran Song, Fan Zhang, and Lingjun Zhang. Ensemble probabilistic wind power forecasting with multi-scale features. *Renewable Energy*, 201:734–751, 2022a.

Yun Wang, Houhua Xu, Runmin Zou, Lingjun Zhang, and Fan Zhang. A deep asymmetric Laplace neural network for deterministic and probabilistic wind power forecasting. *Renewable Energy*, 196:497–517, 2022b.

Edward Wheatcroft. Evaluating probabilistic forecasts of football matches: The case against the ranked probability score. *Journal of Quantitative Analysis in Sports*, 17(4):273–287, 2021.

Robert L. Winkler and Allan H. Murphy. “Good” probability assessors. *Journal of Applied Meteorology*, 7:751–758, 1968.

Robert L. Winkler, Javier Munoz, José L. Cervera, José M Bernardo, Gail Blattenberger, Joseph B. Kadane, Dennis V. Lindley, Allan H. Murphy, Robert M. Oliver, and David Ríos-Insua. Scoring rules and the evaluation of probabilities. *Test*, 5:1–60, 1996.

Keming Yu and Rana A. Moyeed. Bayesian quantile regression. *Statistics & Probability Letters*, 54(4):437–447, 2001.

Keming Yu and Jin Zhang. A three-parameter asymmetric Laplace distribution and its extension. *Communications in Statistics: Theory and Methods*, 34(9-10):1867–1879, 2005.

Lantao Yu, Jiaying Song, Yang Song, and Stefano Ermon. Pseudo-spherical contrastive divergence. In *Advances in Neural Information Processing Systems*, 2021.

## A More details on Covid-19 mortality experiments

### A.1 Converting Hub forecasts

Forecasts in the Hub appear in terms of their quantiles  $[F] = \{F^{-1}(\tau) : \tau \in T\}$ , where  $F$  is the forecasted cumulative distribution function and  $T$  is a discrete set of probability levels, containing evenly-spaced values from 0.05 to 0.95 in increments of 0.05, as well as 0.01, 0.025, 0.0975, and 0.99. Thus a forecast is in fact not a probability distribution but an equivalence class  $[F]$  over probability distributions comprising all distributions that identify on every quantile in  $T$ . In order to compute the loss for a given forecast and observed outcome, we choose a particular representative from the equivalence class  $[F]$ , described as follows. First, we set the representative to have a density which is piecewise linear between  $\min[F]$  and  $\max[F]$  with knots at elements of  $[F]$ . Second, we set the representative to have lower and upper tails (below  $\min[F]$  and above  $\max[F]$ , respectively) of exponential distributions with quantiles matching  $[F]$  on the bottom and top two quantiles in  $T$ , respectively. If  $F$  is the representative of  $[F]$  described above, then we define the loss of the forecast to be  $\ell([F], y) = \ell(F, y)$ . Likewise, the forecast variance was defined as the variance of a random variable with distribution  $F$ . Finally, we discarded forecasts from the Hub with atoms (quantiles which were equal at adjacent probability levels), or forecasts with quantile crossings (quantiles which were out of order at adjacent levels).

### A.2 Standardizing target values

For each location, we estimated the smoothed mean function of the target distribution across time using trend filtering of cubic order (Kim et al., 2009; Tibshirani, 2014) on the observed death counts. Trend filtering is a general-purpose nonparametric smoother that acts similarly to a locally-adaptive regression spline; it is formulated as the solution to a penalized least squares problem, and we used a cross-validation scheme with the one-standard-error rule to choose the

regularization parameter. We then estimated the smoothed variance of the target distribution across dates by applying trend filtering of constant order to the squared residuals from the first step (observed outcomes minus smoothed means), again using cross-validation to select the regularization parameter.